

Elsevier required licence: © <2019>.

This manuscript version is made available under the CC-BY-NC-ND 4.0 license

<http://creativecommons.org/licenses/by-nc-nd/4.0/>

The definitive publisher version is available online at

<https://www.sciencedirect.com/science/article/pii/S2352940719306055?via%3Dihub>

3D printing for membrane separation, desalination and water treatment

Leonard D. Tijing^{1,*}, John Ryan C. Dizon^{2,*}, Idris Ibrahim¹, Arman Ray N. Nisay³, Hokyong Shon¹,
Rigoberto C. Advincula⁴

¹ Centre for Technology in Water and Wastewater, School of Civil and Environmental Engineering,
University of Technology Sydney, 15 Broadway, Ultimo, PO Box 123, 2007 NSW, Australia

² Additive Manufacturing Research Laboratory (AMReL), Department of Industrial Engineering, College of
Engineering and Architecture, Bataan Peninsula State University, City of Balanga, Bataan, 2100, Republic
of the Philippines

³ Department of Mechanical Engineering, College of Engineering and Architecture, Bataan Peninsula State
University, City of Balanga, Bataan, 2100, Republic of the Philippines

⁴ Department of Macromolecular Science and Engineering, Case Western Reserve University, Cleveland,
OH, 44106, USA

*Corresponding authors: L.D. Tijing, leonard.tijing@uts.edu.au, ltijing@gmail.com; J.R.C. Dizon,
johnryancdizon@gmail.com

Abstract

Additive manufacturing or commonly known as 3D printing is driving innovation in many industries and academic research including the water resource sector. The capability of 3D printing to fabricate complex objects in a fast and cost-effective manner makes it highly desirable over conventional manufacturing processes. Recent years have seen a rapid increase in research using 3D printing for membrane separation, desalination and water purification applications, potentially revolutionizing this field. This review focuses on recent advancements in 3D-printed materials and methods for water-related applications including developments in module spacers, novel filtration and desalination membranes, adsorbents, water remediation, solar steam generation materials, catalysis, etc. The emergence of new 3D printers with higher printing resolution, better efficiency, faster speed, and wider material applicability has garnered more interest and can potentially reshape research and development in this field. The promising potential, challenges and future prospects of 3D printing, additive manufacturing, and materials for water resource and treatment-related applications are all discussed in this review.

Keywords: 3D printing; additive manufacturing; membrane; water purification; water treatment; desalination

41 Contents

42	1. Introduction
43	2. Brief overview of additive manufacturing (3D printing)
44	2.1. Additive manufacturing process and techniques
45	2.2. Mechanical properties of 3D-printed materials
46	3. 3D-printed materials for membrane separation, desalination and water treatment
47	3.1. Channel feed spacers
48	3.2. Membranes for filtration and water treatment
49	3.3. Photocatalytic material
50	3.4. Capsules/bio-carriers for wastewater treatment
51	3.5. Sorbents/substrates for oil-water separation
52	3.6. Solar absorbers for solar steam evaporation
53	3.7. Adsorbents/substrates for dye degradation
54	3.8. Adsorbents for heavy metal adsorption
55	4. Challenges of 3D printing
56	4.1. Material and process limitations
57	4.2. Safety and environmental concerns of 3D printing
58	4.3. Industrial upscaling challenges and potential of 3D printing
59	5. Future prospects
60	5.1. Combination of 3D printing + other processes
61	5.2. 4D printing
62	6. Conclusion
63	References

64

65 Abbreviation

66	
67	3D Three-dimensional
68	4D Four-dimensional
69	ABS Acrylonitrile butadiene styrene
70	AM Additive manufacturing
71	BSA Bovine serum albumin
72	CAD Computer-aided design
73	CFD Computational fluid dynamics
74	CLIP Continuous liquid interface production
75	CNT Carbon nanotube
76	DIW Direct ink writing
77	DLP Digital light processing
78	DMLS Direct metal laser sintering
79	DOD Drop-on-demand
80	EDTA Ethylenediaminetetraacetic acid
81	EMB Electron beam melting
82	EPS Expanded polystyrene
83	FDM Fused deposition modelling
84	FFF Fused filament fabrication
85	FO Forward osmosis
86	GO Graphene oxide
87	HIPS High-impact polystyrene
88	LDPE Low-density-polyethylene
89	LMH Liter per square meter per hour
90	MB Methylene blue
91	MBBR Moving bed biofilm reactor

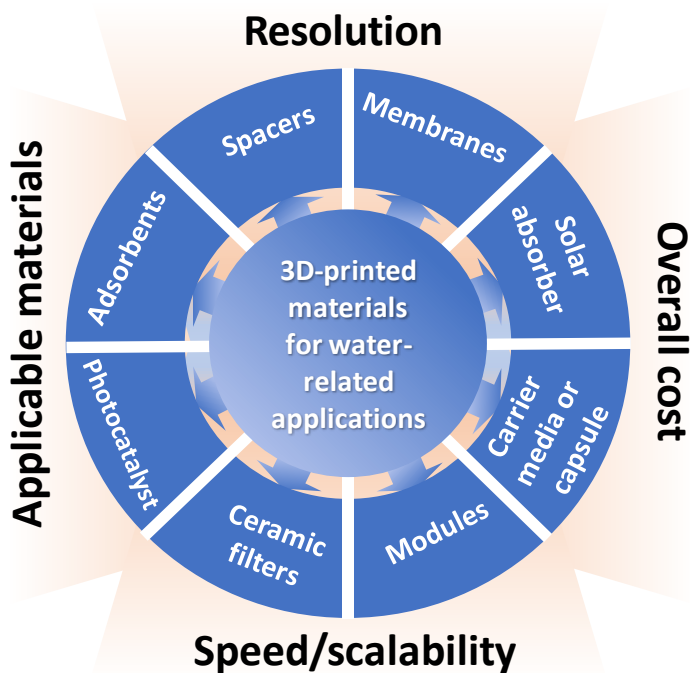
92	MD	Membrane distillation
93	MF	Microfiltration
94	MOF	Metal organic framework
95	MPD	M-phenylene diamine
96	NF	Nanofiltration
97	NFC	Nanofibrillated cellulose
98	NIPS	Non-solvent induced phase separation
99	NP	Nanoparticle
100	PA	Polyamide
101	PBF	Powder bed fusion
102	PC	Polycarbonate
103	PDMS	Polydimethylsiloxane
104	PEEK	Polyether ether ketone
105	PES	Polyethersulfone
106	PLA	Polylactic acid
107	PP	Polypropylene
108	PTFE	Polytetrafluoroethylene
109	PVA	Polyvinyl alcohol
110	PVDF	Polyvinylidene fluoride
111	RO	Reverse osmosis
112	SEM	Scanning electron microscopy
113	SLA	Stereolithography
114	SLM	Selective laser melting
115	SLS	Selective laser sintering
116	SSA	Specific surface area
117	tCLP	Transverse crossed layer of parallel
118	TEM	Track-etched membrane
119	TFC	Thin film composite
120	TMC	Trimesoyl chloride
121	TPMS	Triply periodic minimal surface
122	TPP	Two-photon polymerization
123	UF	Ultrafiltration
124	UV	Ultraviolet
125	VOC	Volatile organic compound
126	WHO	World Health Organization
127	ZIF	Zeolitic Imidazole Framework

128
129
130

1. Introduction

131 The development of new technologies and synthesis of new materials in the last four decades have
132 propelled new frontiers and innovation in addressing a variety of environmental challenges [1]. One of the
133 emerging and promising technological advancements is additive manufacturing or generally known as 3D
134 printing, which is a layer-by-layer fabrication technique [2]. 3D printing can be used to fabricate objects
135 with almost unlimited geometrical constraints, i.e., even complicated designs can be manufactured and
136 assembled by a single pass [3]. This gives a clear advantage when compared with conventional formative
137 manufacturing processes. The emergence of 3D printing technology has enabled rapid prototyping for
138 various engineering and non-engineering applications utilizing a wide range of materials (e.g., polymeric,
139 ceramic, metals, etc.) [4]. Recently, researchers have started looking at 3D-printed materials for membrane
140 separation, water treatment and purification process applications. This stems from the issue of global water
141 resource scarcity, which needs collaborative effort to provide sustainable solutions [5]. These solutions
142 include applications of membrane technology (spacers, modules and membrane fabrication), solar
143 absorbers/steam generation materials, sorbents for oil/water separation, materials for dye degradation

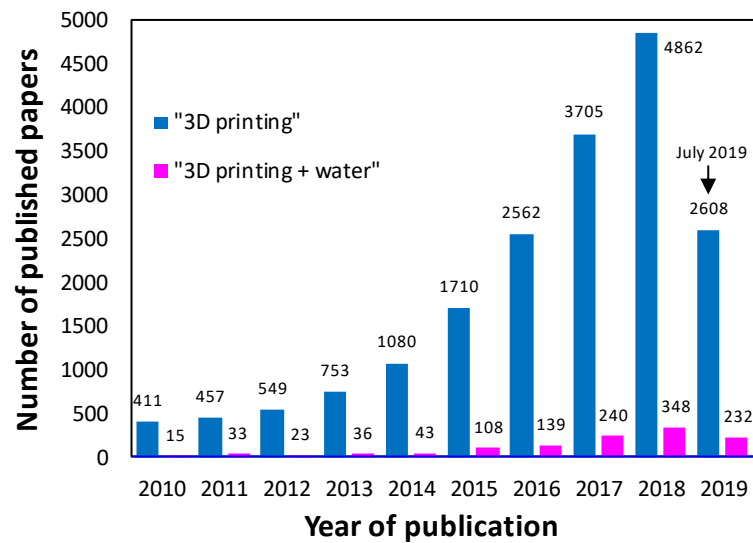
144 and catalysis, etc. (see **Fig. 1**). One of the early applications of 3D printing was on module spacer design
 145 and development utilizing a net-design spacer for membrane separation [6]. Since then, different types of
 146 membrane spacer designs have been reported for applications such as reverse osmosis (RO), ultrafiltration
 147 (UF) [7], membrane distillation (MD) [8], forward osmosis (FO) [9], etc. There have been attempts on direct
 148 fabrication of 3D-printed polymeric [10] and ceramic [11] membranes, or as substrate to membranes [12].
 149 However, due to resolution limitations, direct 3D printing of membranes is still a challenge. Recent
 150 developments in more capable 3D printers have addressed some of these limitations including multi-
 151 material adaptability. Some research groups have reported enhanced solar steam generation performance
 152 from 3D-printed materials, and for other uses such as in water remediation, wastewater treatment, and
 153 adsorption.



154
 155 **Figure 1.** 3D printing has found its way to water-related applications. However, it still faces some issues
 156 on resolution, applicable materials, speed and scalability and the overall cost.

157
 158 The past 10 years have seen a rapid increase in research and development on 3D printing for many
 159 applications as indicated by the exponential increase in publications over the years (see **Fig. 2**). Specifically,
 160 interest on 3D printing for water treatment/purification, and membrane separation applications has been
 161 growing recently as evidenced by the exponential growth of research studies and publications in the
 162 literature. From less than 20 articles published in 2010, papers related to 3D-printed materials for water-
 163 related applications have averaged around 300 papers published annually in the last 3.5 years alone.
 164 Clearly, research interest in this field is rapidly growing. Thus, there is a need to review, discuss and analyze
 165 recent updates of 3D-printed materials work and literature. A few review papers have attempted to provide
 166 new information in this regard, but are only limited to discussions specifically on membranes, or module
 167 spacers. Most published articles have been dedicated only on the discussion of 3D printing technologies
 168 and not their water-related applications [3, 13-15]. In this present review, we emphasize on the latest
 169 progress and developments of 3D-printed materials (polymeric and ceramic) with focus on applications for
 170 membrane separation, wastewater treatment, desalination and water purification especially those
 171 reported in the recent three years. Discussions include the design, fabrication techniques and performance
 172 of 3D-printed materials in water-related applications. General details about additive manufacturing, the
 173 materials used, techniques and related characterizations have also been included. The review concludes

174 with the identification of challenges, and outlining of future prospects of 3D-printed materials for water-
175 related applications.



176

177 **Figure 2.** Number of publications related to 3D printing through the years (data are from Web of Science
178 database with the keywords “3D printing” and “3D printing + water”). Search was refined to only include
179 research and review articles in science and technology field.

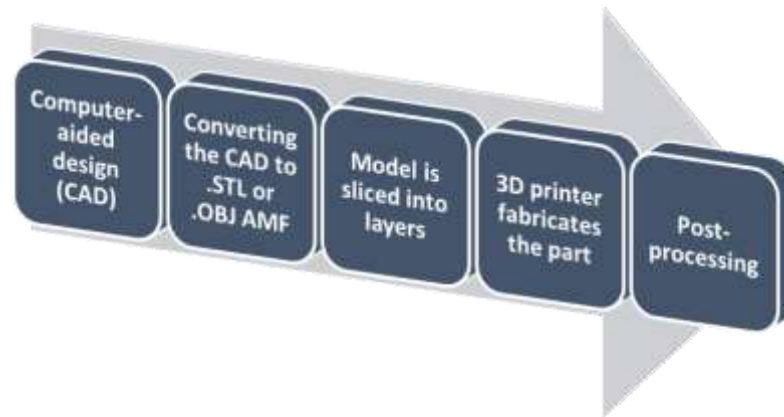
180

181 2. Brief overview of additive manufacturing (3D printing)

182 2.1. Additive manufacturing process and techniques

183 Additive manufacturing (AM) or simply 3D printing is revolutionizing many fields of research and
184 applications. Other terms associated with AM include rapid prototyping, layered manufacturing, direct
185 digital manufacturing, additive fabrication, etc. In this paper, additive manufacturing and 3D printing are
186 interchangeably used. Generally, “additive”, indicates that the fabrication technique is based on printing
187 or adding one layer at a time to produce the 3D structure based on a 3D computer aided design (CAD)
188 model. **Figure 3** shows the general AM process flow. A 3D model of the desired design is first prepared,
189 then subsequently converted to a 3D printer compatible file (usually .STL,.OBJ, or .AMF) [16]. The file is
190 then processed using a slicing software/AM system (usually dedicated to a specific 3D printer), which slices
191 the model in several hundreds or thousands of layers. Various parameters such as printing speed, layer
192 height (resolution), infill, etc. are specified and optimized in the slicing process. The slicing process also
193 converts the .STL file into a file type accepted by a particular 3D printer (G-code) [17]. The sliced file (G-
194 code) is then transferred to the 3D printer, during which, the 3D printer can begin fabricating. After printing,
195 the 3D-printed part usually requires post-processing to remove extra materials or stabilize curing (the
196 extent of which depends on the printer type), and to prepare the part for the desired application [16].

197



198
199

Figure 3. Schematic of the additive manufacturing (3D printing) process flow.

200
201

There are several 3D printing technologies available in the market and are mainly divided into the following categories [3, 13, 17-19] (although there are more):

202
203
204
205
206
207
208
209
210

- 1) Material Extrusion – fused filament fabrication (FFF), fused deposition modeling (FDM), Paste Extrusion
- 2) Powder Bed Fusion – selective laser sintering (SLS), for polymers; selective laser melting (SLM), direct metal laser sintering (DMLS), and electron beam melting (EBM) for metals
- 3) Vat Polymerization – stereolithography (SLA), digital light processing (DLP), two-photon polymerization (TPP) and continuous liquid interface production (CLIP)
- 4) Material Jetting – Polyjet, drop-on-demand (DOD)
- 5) Binder Jetting
- 6) Sheet Lamination

211
212

The most commonly-used 3D printers are the extrusion-based 3D printers, also known as FDM (see **Fig. 4a**) and filament freeform fabrication (FFF), which uses a thermoplastic filament as its printing material [20]. In FFF, the printer prints a 3D object by extruding a melt thermoplastic material following the sliced 3D model [18, 21, 22]. The melt material is positioned layer upon layer until the 3D object/part is created vertically. Stratasys has owned the patent for FDM since 1989 [23]. Common materials for FDM are polylactic acid (PLA), acrylonitrile butadiene styrene (ABS), polycarbonate (PC), and recently, high performance polymers such as polyether ether ketone (PEEK) have also been used. This printing technique is relatively fast and inexpensive, but requires support structures especially for complex shapes [24]. The basic components of a typical FFF/FDM printer include the build platform, heated extrusion nozzle, and the filament material. Paste extrusion printing is similar to FFF/FDM wherein the material is extruded onto the build plate through a nozzle even at room temperature. This method can extrude a highly viscous material, which needs to become solid-like and maintain its shape after extrusion (thixotropic). Different types of materials may be printed including polymer resins, polymer solutions, gels, etc. Postprocessing is usually required [17].

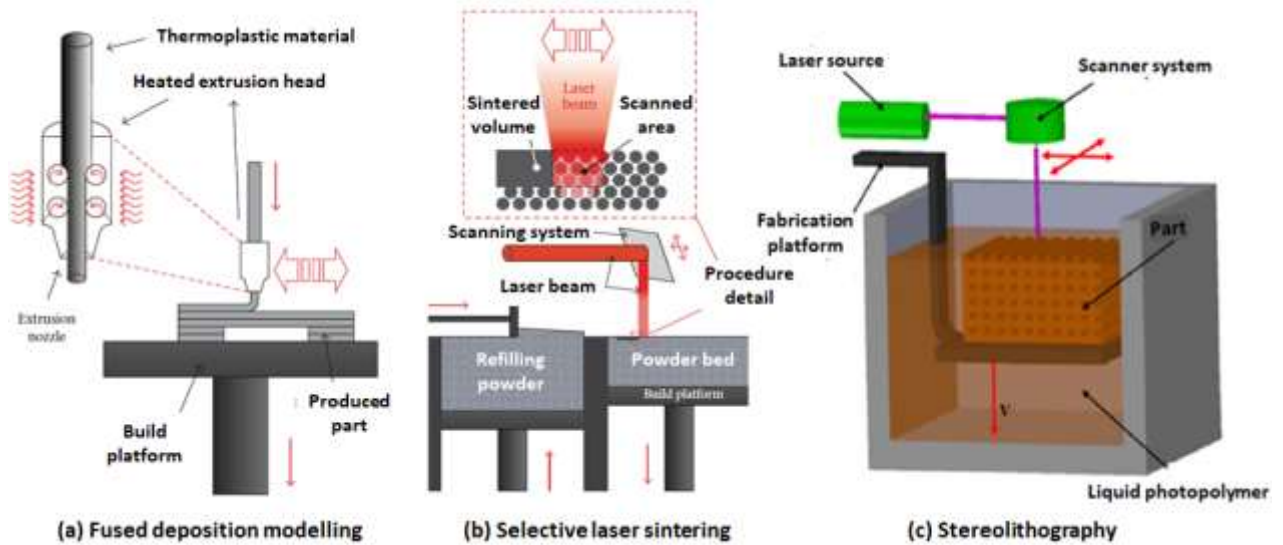
225

226
227

Another common 3D printing technology is SLS additive manufacturing which is a type of powder bed fusion (PBF) process [22, 25]. **Figure 4b** shows a schematic of the SLS printing process. The components of this printing process include the build platform, the printing chamber (including the powder bed), powder reserve chamber (including the refilling powder), and the laser beam (source). The printing chamber and powder reserve chamber are initially heated to a certain temperature (below the melting point of the material). And then, a bed of powder is partially targeted (sintered) by a laser beam in order to fuse the powder materials into a predefined 2D shape/contour (based on the 3D model) on the surface of the powder bed. The top surface of the powder bed is refilled with a fresh layer of powder (from the refilling powder chamber) covering the sintered cross-section [22, 26]. This process is repeated until the desired 3D object is completed. Many types of materials including polymers, ceramics, metals and composites may be used as printing material in this 3D printing technology [25-27]. It is possible to easily print complicated shapes with SLS as this process does not need structural support since the powder bed acts as support for

237

238 the printed item [28, 29]. Laser power, powder particle size, scan speed and scan spacing are the factors
 239 that define the quality of an SLS print [30].
 240
 241



242
 243
 244 **Figure 4.** Schematic representation of the most common 3D printing techniques: (a) Fused deposition
 245 modelling (FDM) (adapted from [25]); (b) selective laser sintering (SLS) (adapted from [25]), and; (c)
 246 stereolithography (SLA) (adapted from [22]).
 247
 248

249 Stereolithography (SLA) is an additive manufacturing process wherein a part is created by selectively curing
 250 a (liquid) photosensitive thermoset polymer resin layer-by-layer using an ultraviolet (UV) laser beam, as
 251 shown in **Figure 4c**. This was the first AM technique developed [18]. The build platform is initially positioned
 252 in the vat with liquid photopolymer resin, at a distance of one layer height from the surface of the liquid
 253 resin. Then, the UV laser creates the next layer by selectively curing (polymerizing) the resin. The laser beam
 254 follows a predetermined path based on the cross-sectional area of the 3D model. After curing a layer, the
 255 build platform moves down (in other configurations, moves up) and the sweeper/wiper recoats the surface
 256 with a new layer of resin. This process is repeated until the part is complete. Postprocessing may be needed
 257 in order to achieve optimum thermo-mechanical properties. With this technique, high resolution could be
 258 achieved [18]. Similar to SLA, DLP uses photopolymers as 3D printing materials. The only difference is that
 259 DLP uses a different light source, e.g. an arc lamp with a liquid crystal display panel or micromirrors. This is
 260 then applied to the entire surface of the vat of thermoset photopolymer resin in a single projection,
 261 technically making it a faster process than SLA [18].

262 The 3D printing technologies presented here provides insights representing almost all 3D printing processes
 263 used for rapid prototyping. Specifically, representative 3D printing technologies using different printing
 264 materials (i.e. solid-based, powder-based and liquid-based) have been discussed. Other AM technologies
 265 may be found from recent publications [17-19]. A comprehensive summary covering most of the AM
 266 technologies and materials as well as the companies manufacturing them have been presented by Low et
 267 al. [13].
 268

269 **2.2. Mechanical properties of 3D-printed materials**
 270

271 For practical applications, several properties especially the mechanical properties of 3D-printed materials
 272 have to be considered. One major issue is the mechanical anisotropy which is different for various printing
 273 technologies, and is dependent on raster (layer) orientation. Due to poor interlayer bonding, weak tensile
 274 properties are observed when the 3D-printed samples are loaded along the build directions. Other factors

275 to be considered which affect the mechanical properties of 3D-printed parts particularly FDM include layer
 276 thickness and air gap. Under compression loading, lower strength has been observed for parts having a
 277 transverse-build direction as compared with the sample having an axial build direction. The compressive
 278 strength of the part is less than 90% of the injection molded part. For SLA, build orientation and layer
 279 thickness affect the mechanical property of parts. Particularly, tensile strength increases with increasing
 280 layer thickness, while the impact strength and flexural strength decreases. For SLS, the mechanical
 281 properties depend on input energy, scan spacing, refresh rate, part orientation, feedstock uniformity,
 282 microstructure evolution, layer thickness, part bed temperature, hatch pattern, and laser beam speed.
 283 Mechanical anisotropy is also found with SLS-printed parts. Actually, there is varying anisotropy in 3D-
 284 printed parts with different printing technologies. **Table 1** presents the different factors affecting the
 285 mechanical properties of 3D printed materials fabricated by various techniques. A comprehensive
 286 discussion on the mechanical properties of 3D-printed parts is reported in our previous paper [18].

287
 288
 289
 290

Table 1. Factors affecting the mechanical properties of various 3D printing technologies

3D printing technology	Factors affecting the mechanical properties
Fused Deposition Modelling (FDM)	Build direction, layer thickness, air gap
Stereolithography (SLA)	Build orientation and layer thickness
Selective Laser Sintering (SLS)	Input energy, scan spacing, refresh rate, part orientation, feedstock uniformity, microstructure evolution, layer thickness, part bed temperature, hatch pattern, and laser beamspeed
Digital Light Processing (DLP)	Build direction, pixelation
Three-Dimensional Printing (3DP)	Internal structure, binder content, sintering temperature, binder adsorption, mechanical locking, bonding between adjacent powders and adjacent layers
Polyjet	Printing orientation, post-processing, part spacing along the y-axis, aging
Laminated Object Manufacturing	Printing orientation

291

3. 3D-printed materials for membrane separation, desalination and water treatment

292

293 In recent years, AM (3D printing) has provided remarkable advancements in membrane module design,
 294 composite membrane fabrication, development of oil-water separation and wastewater treatment
 295 materials, etc. despite the limitations on cost, speed, printing resolution and material selection. Increasing
 296 number of research groups are utilizing 3D printing for designing complicated structures with ease of
 297 prototyping and tests for various water-related applications. **Table 2** lists various water-related applications
 298 as reported in literature using 3D printing to prepare all or parts of the main materials used for various
 299 water-related applications. From the table, it can be deduced that FDM, SLS, SLA and polyjet are the most
 300 commonly used methods to 3D-print their materials depending on the target applications. Discussions on
 301 each application are detailed in the following sub-sections.

302

303 **Table 2.** Comprehensive list of various materials prepared by 3D printing for water-related applications
 304 including details on the materials used, the 3D printing technique, the printed part and their corresponding
 305 applications (Abbreviations: SLS – selective laser sintering; FDM – fused deposition modeling; DLP – digital
 306 light processing; FFF – fused filament fabrication; SLA – stereolithography; RO – reverse osmosis; MD –
 307 membrane distillation; MF – microfiltration; NF – nanofiltration; UF – ultrafiltration; FO – forward osmosis).

Technology/application	3D-printed part	Material	3D printing technique	Refs
(a) Membrane separation				
<i>Spacers</i>				
RO, UF	Spacer	Polyamide 12 (PA 2202 (black) Thermoplastic)	SLS	[7]
MD	Spacer	Polyamide 12 (PA 2202 (black) Thermoplastic)	SLS	[8, 31, 32]
Filtration	Spacer	Polypropylene (PP)	SLS	[33]
Filtration	Spacer	Polyamide 12 based white powder PA2200	FDM SLS Polyjet	[34]
NF, RO	Spacer	Urethane acrylate polymer	Polyjet	[35]
MF	Vibrating spacer	Solid polyamide	SLS + Simulation by COMSOL	[36]
UF	Spacer	Liquid resin (Acrylate monomer)	DLP	[37]
FO	Spacer	Polypropylene, Polylactic acid (PLA), Acrylonitrile butadiene styrene (ABS)	Polyjet, FDM	[9]
Filtration	Spacer	-	SLS	[6]
Filtration	Spacer	-	SLS	[38]
RO, UF	Spacer	Acrylonitrile butadiene styrene (ABS)	FDM	[39]
UF	Spacer	-	SLA	[40]
UF	Spacer	-	Polyjet	[41, 42]
UF	Spacer	acrylate monomer	DLP	[43]
<i>Membranes</i>				
RO, NF	Thin film composite membrane	Fluorinated diamine incorporated into an m-phenylenediamine-based polyamide	Inkjet printing + interfacial polymerization	[44]
UF	Composite Membrane	ABS-like substrate	Multijet printing	[12, 45]
Advanced water treatment	Biocatalytic membrane	Polyvinyl alcohol (PVA) + yeast cells	Inkjet printing	[46]
-	Membrane	PLA, Polybenzimidazole (PBI), PVA	Solvent cast printing (SCP), FFF	[47]
Filtration	Ceramic membrane	Kankara clay powder + maltodextrin powder	Inkjet	[11]
RO	Thin film composite membrane	metaphenylene diamine (MPD) and trimesoyl chloride (TMC)	Electrospraying (for the active layer)	[48]
Oil-water separation	Membrane	Polysulfone	SLS	[49]
Oil-water separation	Membrane	Polyamide 12 (PA 2200)	SLS	[50]

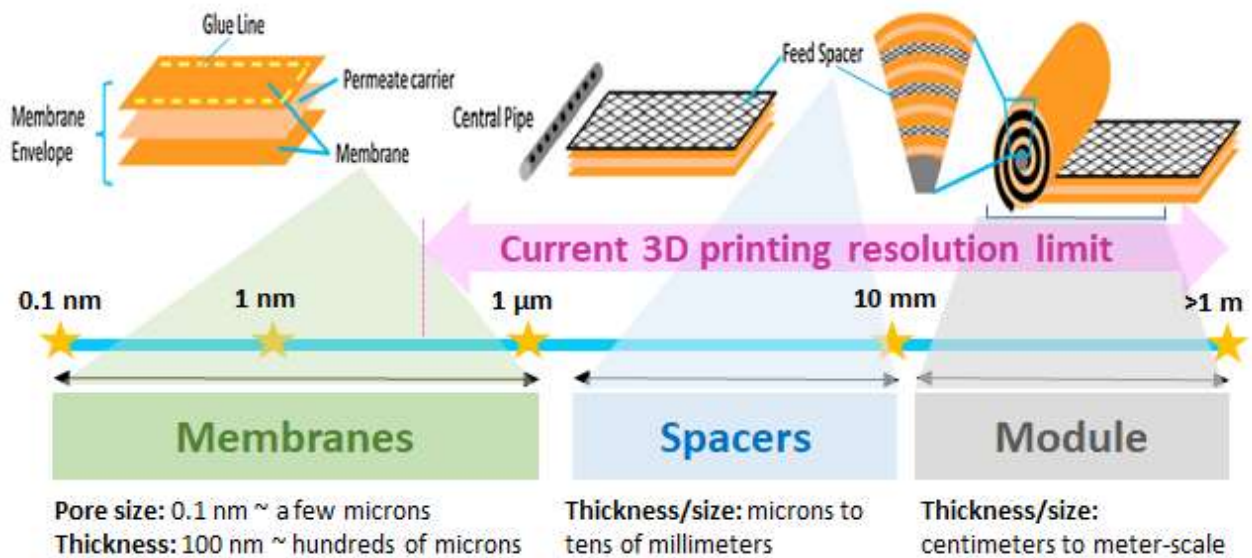
Anion exchange	Anion exchange membrane	Quaternized poly(DUDA-co-PEGDA-co-VBC)	-	[51]
Gas-liquid contactors	Moulded membrane	Polydimethylsiloxane (PDMS)	DLP	[10]
(b) Wastewater treatment				
Degradation of pharmaceuticals	Capsules filled with ferrate	PVA	Lab-made printer	[52]
Biofilm reactor	Fullerene-inspired bio-carrier media	Nylon	SLS	[53]
Moving bed biofilm reactor (MBBR)	Biofilter media carrier	Liquid acrylate-based monomer resin	Polyjet	[54]
(c) Solar steam generation				
Desalination	Solar evaporator with concave structure	Nanofibrillated cellulose (NFC) with graphene oxide (GO) and carbon nanotubes (CNT)	FDM	[55]
Desalination	Jelly-fish like solar evaporator	Porous carbon black/graphene oxide + aligned GO pillars + expanded polystyrene	Vertical 3D printing	[56]
	Hybrid aerogel membrane	2D carbon nitride	Direct writing	[57]
(d) Adsorption/dye degradation				
MB removal	MOF composite	ABS coated with Cu-BTC (BTC = benzene tricarboxylic acid) metal-organic frameworks	FDM	[58]
Rhodamine B degradation	Zeolitic Imidazole Framework (ZIF-67)/ polymer mixed matrix on 3D printed device	-	SLA	[59]
(e) Oil-water separation				
Oil-water separation	Egg-beater superhydrophobic structure	E-glass with carbon nanotubes	Immersed surface accumulation based 3D (ISA-3D) printing	[60]
Oil-water separation	Oil skimmer mesh	-	SLA	[61]
Oil-water separation	Ceramic mesh	Alumina	DLP	[62]
Oil-water separation	Porous membrane	PDMS	DLP	[63]

308

309 3.1. Channel feed spacers

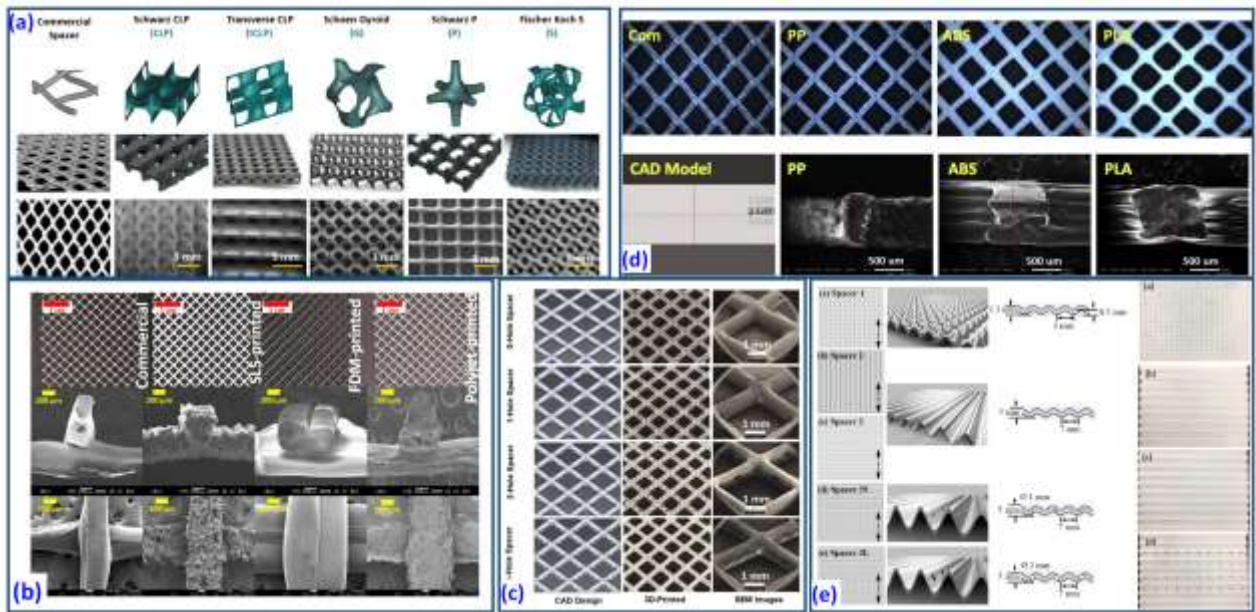
310 For many membrane separation applications especially using spiral wound membranes (SWM), feed
311 channel spacers serve a very significant role in ensuring continuous flow and recirculation as well as fluid
312 mixing [64]. Feed spacers come in various designs with the goal of enhancing turbulence, maintaining
313 constant space (mechanical support) for fluid to pass through, reducing fouling formation, and preventing
314 damage of the active layer of the membrane [3]. **Figure 5** (top image) shows the schematic diagram of how
315 the spacer is placed in the module and the comparative dimensional requirements for various parts of the

316 membrane module - from the membranes, spacers, and module sizes. As the spacer needs to be rolled up,
 317 it needs a balance of stiffness and flexibility, as well as good chemical resistance, thus commercial spacers
 318 are usually made of polypropylene (PP) [33]. Good spacer design is important as dead zones create
 319 situations for particle deposition leading to fouling that reduces mass transfer rate. Different spacer designs
 320 with various characteristics have been tested to limit dead zones and to determine its effect on mass
 321 transfer, pressure drop, and fouling [64, 65]. However, the complex spacer design and geometry can pose
 322 manufacturing challenges using conventional techniques such as heat extrusion, moulding or vacuum
 323 foaming. Hence, the potential of 3D printing in fabricating complex-design feed spacer is considered due
 324 to its ability to fabricate any simple or complicated geometries.



325
 326 **Figure 5.** Top image shows the schematic of the spiral wound membrane (SWM) module components
 327 including the feed spacer (modified from [33]). The bottom image illustrates the comparative dimensions
 328 of the different parts of a membrane unit, and the current resolution limitations of 3D printing (modified
 329 from [3]).

330
 331 Researchers have reported various spacer designs and geometries using 3D printing since the first report
 332 in 2014 [3, 66]. Among the spacer designs include triply periodic minimal surfaces, multi-layered spacer
 333 structures, herringbone and helices, twisted tapes, ladders, etc. [3]. These spacers were fabricated using
 334 different types of 3D printing techniques and printing materials. **Table 3** and **Figure 6** show a summary of
 335 the various 3D-printed feed spacers reported to date. Most of the spacers were mainly printed by SLS, FDM,
 336 DLP, and polyjet methods. A series of research work by Arafat et al. [7, 8, 32] investigated various 3D-
 337 printed spacer designs for membrane performance enhancement and fouling control (see **Fig. 6a**). For
 338 example, they [7] proposed a triply periodic minimal surface (TPMS) spacer design to enhance flux
 339 performance and fouling resistance of RO and UF processes. Their TPMS design was based on its success
 340 for use in heat exchanger units. Desalination tests showed flux enhancements of 15.5% (for brackish water
 341 RO) and 38% (for UF) when compared with those using commercial polypropylene feed spacer. Biofouling
 342 formation was reduced using TPMS while minimizing pressure drop across the membrane. The same TPMS
 343 spacer design was further tested for MD scaling control [8] and organic fouling [32] in their subsequent
 344 studies. Using calcium sulfate (at 1900 mg/L) as model foulant [8], the TPMS (particularly tCLP) achieved
 345 50% higher flux and less membrane scaling compared to a commercial spacer. However, pressure drop was
 346 found to be higher. Combining the tCLP and gyroid design into one spacer maintained high flux, low
 347 membrane scaling, but at a lower pressure. Interestingly, it was noted that the micro-surface roughness of
 348 the TPMS enhanced scale formation on the spacer itself. But the same TPMS design also resulted to lower
 349 organic fouling formation [32]. In order to maintain high recovery rate, fouling pre-treatment and cleaning-
 350 in-place for both membrane and spacers are necessary.



351
 352 **Figure 6.** Some example designs of 3D-printed spacers reported in literature: (a) Various designs of 3D-printed triply periodic minimal surfaces (TPMS) spacers: representative volume
 353 element (top row), photographic images (middle row), SEM images (bottom row) [7]; (b) photographic and
 354 SEM images of different 3D-printed spacers printed by SLS, FDM and polyjet in comparison with the
 355 commercial net spacer [34]; (c) CAD models, and the photographic and SEM images of the 3D-printed
 356 spacers with 0-hole, 1-hole, 2-hole and 3-hole spacer [37]; (d) Stereo fluorescence images of commercial
 357 and 3D-printed spacers made of PP, ABS and PLA with various designs, and the corresponding SEM
 358 images of the 3D-printed spacers and a CAD model for thickness comparison; (e) Different designs of polyamide
 359 3D-printed spacers with repeating hill-like structures and wave-like protrusions with and without
 360 perforations (vibration capability).
 361

362
 363 Tan et al. [33] prepared a net-type feed spacer made of polypropylene (PP) by the SLS method. They
 364 investigated the optimum building temperature and process parameters in 3D printing the PP spacer. The
 365 accuracy of printing and mechanical properties of the printed part were evaluated. Results indicated that
 366 the energy density (laser power, scanning speed and scanning distance) used was proportional to the
 367 Young's modulus, and ultimate tensile strength. Meaning, the higher energy density, the higher the Young's
 368 modulus and ultimate tensile strength of the printed part. However, the accuracy of the dimensions was
 369 found to have a correlation with the Young's modulus of the PP material. In their subsequent study, [34]
 370 three 3D-printing methods were compared, namely, SLS, polyjet and FDM on their geometry and surface
 371 finish. Their membrane performance and fouling properties were also considered (see **Fig. 6b**). Regardless
 372 of the printing method it was found that the 3D-printed spacers maintained superior mass transfer
 373 performance at fixed power consumption and critical flux when compared with a commercial spacer. In
 374 terms of printing accurateness, their tests showed a preference of: polyjet>SLS>FDM. Further consideration
 375 can be made on the; (a) geometric printability, (b) model to part accuracy, and (c) surface finish when
 376 fabricating spacers.
 377

378 Kerdi et al. [37] tested three symmetric perforated spacer designs (1-hole, 2-hole and 3-hole) fabricated by
 379 DLP 3D printing on their hydrodynamic performance and filtration efficiency in ultrafiltration test. Direct
 380 numerical simulation was carried out to further enhance the understanding of their performance and
 381 mechanism. They hypothesized that the perforations in the new design would increase the shear stress at
 382 the membrane surface thereby reducing fouling, and at the same time reduce the net pressure in the
 383 module. Under ultrafiltration tests, the perforated 3D printed membranes compared to non-perforated
 384 ones showed better filtration performance due to the presence of micro-jets as induced by the perforations

385 through elimination of dead zones. The 1-hole spacer obtained the best performance among all designs,
 386 showing 75% (under constant pressure) and 23% (under constant feed flow) improvements in permeate
 387 flux, and had the cleanest membrane surface (less fouling). The 3-hole spacer showed high reduction in
 388 pressure drop (54%) but did not translate to increased permeation flux. Also, increasing the number of
 389 perforations resulted to more fouling due to reduction in unsteadiness of water flow. Overall, the three
 390 different perforated designs resulted in thinner fouling formation compared to 0-hole spacer. The optimum
 391 spacer design was concluded to be the 1-hole spacer based on the conditions of this study. In a similar
 392 manner, Ali et al. [43] utilized DLP to print their spacer with column designs. With their design, they aimed
 393 to increase the clearance between the filament and the membrane, while maintaining the same flow
 394 channel thickness. The column type nodes were added to act as vortex shading structures. Numerical
 395 analysis showed less pressure drop using their 3D printed spacer, including lesser dead zones as also proven
 396 by their experimental results. When compared with standard commercial spacer, the 3D-printed spacer
 397 with column design obtained two orders of magnitude lower specific energy consumption than the
 398 standard spacer. Using polyjet and FDM 3D printing, Yanar et al. [9] investigated the mechanical properties,
 399 flux and fouling performance under FO operation of three diamond-shaped spacer made from ABS,
 400 polylactic acid (PLA) and PP (see Fig. 6d). The reference spacer was a commercial PP spacer with diamond
 401 shape design. The study found that the material and the kind of 3D printing technique used have a
 402 corresponding effect on the spacer properties and performance. PP and PLA were found to have best FO
 403 performance, particularly in terms of reverse solute flux and fouling resistance. Fouling resistance was
 404 found much better when using PLA (10% less) when compared with the commercial PP spacer. In another
 405 study, vibrating 3D-printed spacers with unique designs (see Fig. 6e) were prepared by Tan et al. [36] using
 406 SLS method together with COMSOL simulation. The aim was to determine the effect of spacer configuration
 407 and vibration configuration on fouling control in a submerged microfiltration system environment. It was
 408 concluded that the spacer design and configuration affected the extent of fouling control performance,
 409 with wavy design outperforming the hill-structure design. Also, smaller perforations performed better
 410 compared to larger perforations.

411
 412 Based on literature, feed spacer materials have been one of the most researched materials for 3D printing
 413 application in recent years especially for desalination and water treatment. This is primarily due to the
 414 suitable printable resolution in current 3D printers, wherein complex designs can easily be fabricated. Most
 415 results on 3D-printed spacers indicate better performance in terms of flux performance, control of fouling,
 416 and even improving hydrodynamic flow compared to commercially available spacers. However, the surface
 417 finish needs further improvement for many 3D printed spacers. In addition, availability of more materials
 418 for 3D printing with good mechanical and surface properties in compartmentalized modules is attractive.

419
 420
 421 **Table 3.** Various 3D-printed feed spacers reported in literature with details on the design/geometry,
 422 materials used, 3D printing technique and their intended applications (Abbreviations: RO – reverse
 423 osmosis; MD – membrane distillation; NF – nanofiltration; UF –ultrafiltration; FO – forward osmosis;
 424 DCDM – direct contact MD).

Spacer design and material	3D printing technique	Application	Remarks	Ref
Triply periodic minimal surfaces (TPMS), tCLP and Gyroid	Selective laser sintering (SLS)	MD	- Scaling (calcium sulfate) control in DCMD. - 50% higher flux for tCLP compared to commercial spacer. - Lesser scaling for membranes using TPMS spacer.	[8]
Triply periodic minimal surfaces (TPMS)	Selective laser sintering (SLS)	RO, UF	- Compared with a commercial membrane, TPMS spacers showed flux enhancements of	[7]

			<p>15% for brackish water RO and 38% for UF.</p> <ul style="list-style-type: none"> - Biofouling was found to be lesser using TPMS. 	
Triply periodic minimal surfaces (TPMS) – gyroid and tCLP	Selective laser sintering (SLS)	DCMD	<ul style="list-style-type: none"> - 50-65% flux enhancement when using TPMS compared to commercial membrane. - Gyroid design: better organic fouling control - 99% salt rejection and better permeate quality. 	[32]
Polypropylene net structures	Selective laser sintering (SLS)	Spiral wound membrane modules for water industry	<ul style="list-style-type: none"> - Investigated the printability of PP polymer for net-type spacer structures. - Found that SLS can successfully print PP into spacers. - Higher printing energy density used resulted to better mechanical properties. - Found there is correlation of accuracy of dimensions and the resulting Young's modulus. 	[33]
Polyamide 12, ABSplus™, Acrylic based monomer VeroClear net spacers	FDM, SLS and Polyjet	Spiral wound membrane modules	<ul style="list-style-type: none"> - Compared three 3D printing techniques: FDM, SLS and polyjet for their printing ability - All spacers by the three techniques showed better mass transfer at fixed power consumption and critical flux 	[34]
Urethane acrylate polymer - Modified filament angle, modified mesh size, and combination of both designs	Polyjet	RO and NF	<ul style="list-style-type: none"> - Results: 3D printing can copy the current spacers used in practice with similar results in hydrodynamics, pressure drop and biofouling. - Modifying the design slightly (filament angle, mesh size, or both) from commercial spacer using 3D printing can result in lesser pressure drop and biofouling. - FDM and SLA: found not suitable printing techniques for the present spacers 	[35]
Symmetric perforated spacers, Acrylate Monomer	Digital light processing (DLP)	UF	<ul style="list-style-type: none"> - Hydrodynamic changes, filtration tests and fouling. - Perforated spacers lowered the net pressure drop (with 3-hole having lowest pressure drop). - 1-hole spacer was the most efficient in terms of permeate flux enhancement and least fouling. 	[37]

Acrylonitrile butadiene styrene (ABS), polypropylene (PP), and natural poly(lactic acid) (PLA) – diamond-shape feed spacer	PolyJet, FDM	FO	<ul style="list-style-type: none"> - Comparison of performance of three materials for 3D printing of diamond-shaped spacers: ABS, PP and PLA. - Similar results for water flux, but the 3D printed spacers gave better reverse solute flux and fouling resistance compared with commercial spacer. - PP and PLA had best performance with PLA as having 10% less fouling. 	[9]
Acrylate monomer column type design	Digital light processing (DLP)	UF	<ul style="list-style-type: none"> - Column spacer reduced the pressure drop by three times and doubled the specific water flux. - Less bioaccumulation on the column type spacer - Specific energy consumption - two folds lower than standard spacer 	[43]

425

426

427

3.2. Membranes for filtration and water treatment

428

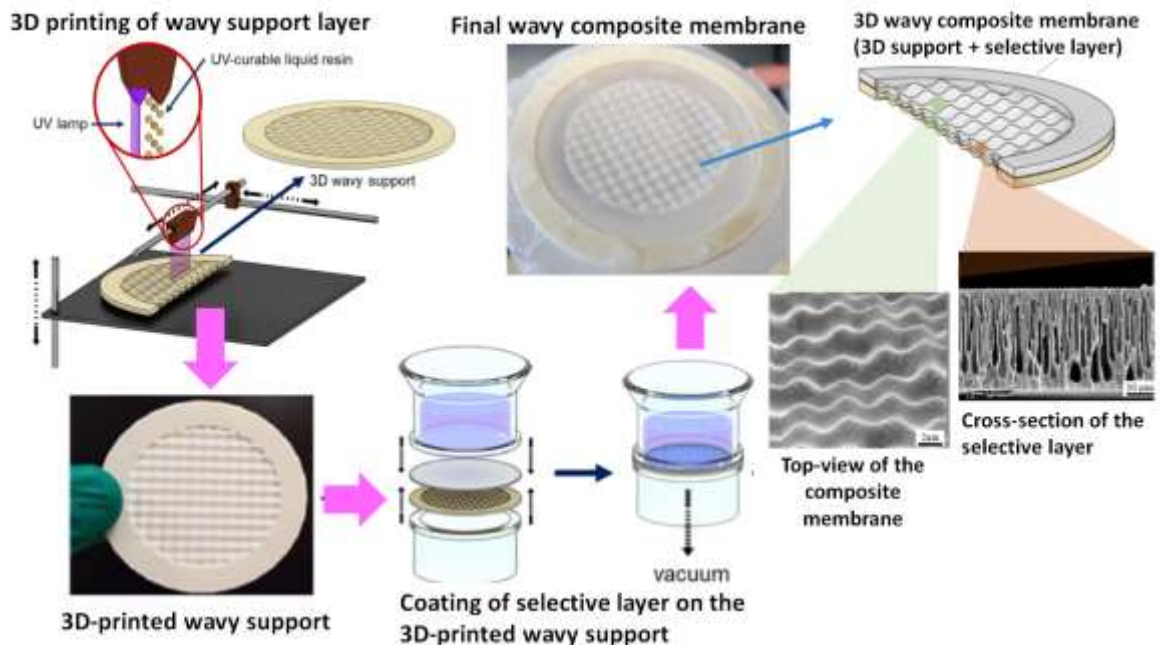
Membrane technology is rapidly advancing and has replaced many conventional water treatment processes due to its high efficiency and cost-effectiveness [67, 68]. Majority of the membranes used are made of polymers but ceramic membranes are also utilized. Conventional polymeric membrane fabrication techniques include phase inversion [69], hollow fiber spinning [70], stretching, and extrusion. Increasing number of studies have also focused on the electrospinning technique for various desalination and water treatment applications [71-73]. The capability of 3D printing to precisely fabricate hierarchical structures and scale is promising for membrane fabrication. However, due to resolution and materials limit, 3D printing is not yet widely investigated for direct polymeric membrane development [3]. Most available 3D printers are not yet able to efficiently print below submicron resolution, where membrane pores are usually in that range. In addition, some membrane applications require specific types of material characteristics and wettability (hydrophilic or hydrophobic), rendering it a challenge as current 3D printers are limited to their applicable/printable materials. Still, a few research groups have started to demonstrate the potential of 3D printing for membrane-related fabrication, usually in the form of composite membrane, i.e., with 3D-printing used for the substrate, and other techniques to fabricate the active layer.

442

Shimerry et al. [12] investigated the performance and anti-fouling behavior of a composite membrane composed of 3D-printed ABS-like support layer (with flat and wavy surface structures) by multijet printing and a thin polyethersulfone (PES) selective layer. The PES layer was casted on top of the support layer via phase inversion. **Figure 7** shows the schematic of the fabrication process and the photographic and SEM images of their composite membrane. The authors carried out ultrafiltration tests to investigate the performance of the fabricated membrane based on their permeation, oil rejection and anti-fouling behaviour. Fouling, which is the deposition of unwanted materials on/in the membranes, is a major challenge for all membrane separation processes as it reduces the efficiency, performance and life of a membrane [74]. For fouling test, oil-in-water emulsion was used as model foulant to check the fouling resistance of the 3D-printed composite membrane. Under 1 bar transmembrane pressure, results indicated better permeability for the wavy membrane (30% higher) compared to the flat membrane, while maintaining high oil rejection (96%). The wavy membrane also has less fouling and proved easier to clean even with water only than the flat membrane. The authors claimed composite membranes have

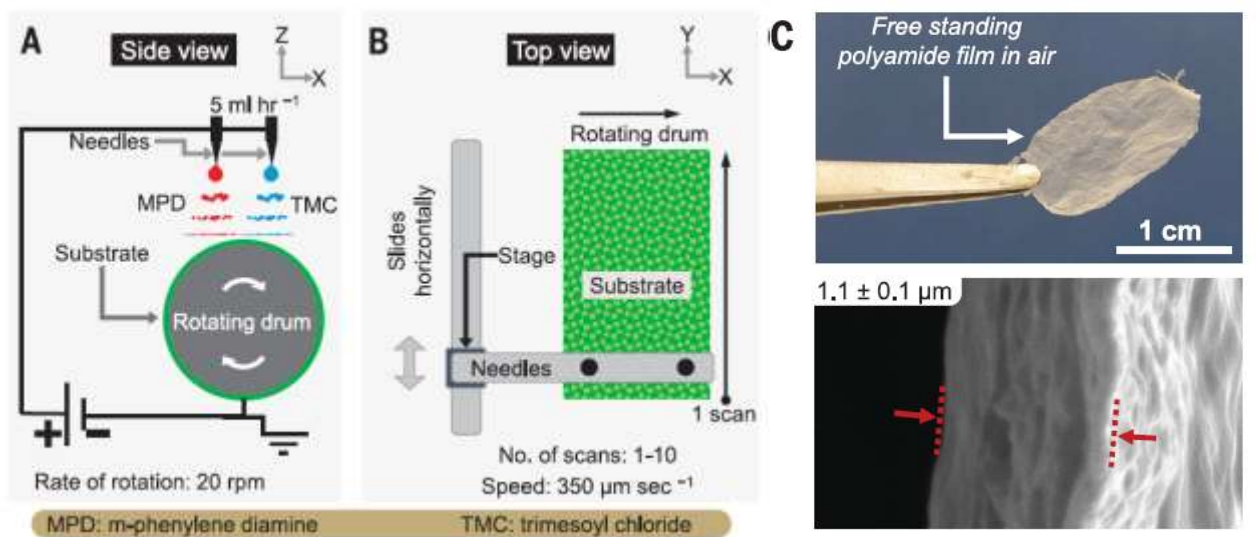
454

455 comparable results with PES mixed matrix membranes reported in literature but was much better than
 456 pure PES membranes. Their subsequent report [45] indicated better bovine serum albumin (BSA) fouling
 457 resistance of their composite membrane with wavy support, even retaining >80% initial permeance after
 458 10 test cycles with water as the only cleaning agent. Though initial results are promising, the report lacked
 459 information on the potential delamination of the selective layer for long-term operation, and the challenge
 460 of upscaling or modulation as the 3D-printed support layer may be too stiff and not easy to bend for module
 461 preparation.



462
 463 **Figure 7.** Schematic of the composite membrane: support layer was 3D-printed with wavy design while
 464 the selective layer on top was first casted by non-solvent induced phase separation (NIPS), then the
 465 casted membrane is attached on the 3D-printed support by vacuum filtration (figure was modified from
 466 [12] and [45]).

467
 468 Compared with other common 3D printing techniques, Chowdhury et al. [48] demonstrated the potential
 469 of electrospinning as a variant of 3D printing to fabricate a very thin polyamide selective layer of a thin film
 470 composite (TFC) RO membrane. TFC membranes are composed of a very thin and dense polyamide
 471 selective layer, a middle support layer, and a thick backing layer for mechanical support. The most
 472 important part of the membrane is the ultrathin selective layer, as this is where the separation process
 473 takes place. Though conventional TFC membranes are considered as state-of-the-art membranes for
 474 desalination with high permselectivity, the synthesis of the selective layer is not easy to control. Most
 475 especially, the thickness and roughness of the selective layer are important to affect the flux, selectivity
 476 and fouling tendency of the membrane. To precisely control the selective layer thickness, Chowdhury et al.
 477 [48] directly deposited monomers (m-phenylene diamine (MPD) and trimesoyl chloride (TMC)) by
 478 electrospinning onto a UF substrate to form the polyamide layer. **Figure 8** shows the schematic of the
 479 electrospinning system, the fabrication process and the example images of the fabricated selective thin
 480 polyamide layer and its corresponding scanning electron microscopy (SEM) image. Since the
 481 electrospinning produced droplets on the substrate surface in an additive way, its thickness could be
 482 controlled more precisely as well as the resulting roughness. With this approach, they were able to control
 483 the thickness up to 15 nm with resolution of around 4 nm, and roughness resolution of up to 2 nm. The
 484 permselectivity and flux performance were also found to be comparable with a commercial TFC membrane.
 485 It is noted though that this process is not in the truest sense of 3D printing process as there was no 3D CAD
 486 models made, and no slicing done on the model for printing.



488

489 **Figure 8.** (a, b) Schematic of electrospaying process for printing polyamide films; (c) photographic image
 490 of a free-standing electrospayed polyamide thin film and its corresponding SEM cross-sectional image
 491 (adapted from [48]).

492

493 Yuan et al. [50] prepared a ZIF-L decorated 3D-printed polyamide (PA) membrane substrate (SLS-printed)
 494 with superhydrophobic and underwater superoleophobic surface. Two steps were involved in the
 495 preparation of the composite membrane. The first was the synthesis of two kinds of uniquely-shaped ZIF-
 496 L particles and the second step was the deposition of the ZIF-Ls on the 3D-printed PA substrate. Upon the
 497 application of the 3D-printed composite membrane in oil-water separation, it achieved a separation
 498 efficiency of over 99% and an oil flux of 24,000 LMH.

499

500 Among various 3D printing techniques, the liquid-based DLP was used by Wessling's group to print directly
 501 a polydimethylsiloxane (PDMS) membrane for gas-liquid contact based on Schwarz-P triple periodic
 502 minimal surface (TPMS) design. This study was considered the first report of 3D printed membrane. PDMS
 503 has a high permeability for various gases. However, it has shown a 15% lower permeability due to its
 504 thickness of 840 μm and higher crosslinking density in the printed membrane [13, 75]. The same group has
 505 reported an indirect printing of PDMS with complicated geometries using a sacrificial mold that serves as a
 506 template for membrane design and fabrication. The membrane has shown an improvement in terms of
 507 mass transfer, but still thicker than conventional membranes.

508 Mecham et al. proposed the production of thin membranes through the continuous liquid interface
 509 production (CLIP) method based on a DLP system for resin formulations. This method has capability of
 510 printing objects continuously instead of layer-by-layer thereby enhancing the printing speed. The group
 511 reported on the potential of this method in production of thin supported membrane structures for water
 512 and gas separation by using a wide variety of polymers. They also addressed the potential of exploring the
 513 influence of process parameters on the permeation and separation characteristics [76]. Recently, a study
 514 using an enhanced CLIP method was reported by Lin's group. The method utilizes a track-etched membrane
 515 (TEM) which serves as the oxygen-permeable window during the process. Due to high oxygen permeability
 516 of TEM, the printing speed of the manufacturing process is measured up to 800 mm per hour using pure
 517 oxygen and 470 mm per hour even when using air [77]. Hwa et al. [11] investigated the performance of a
 518 3D-printed Kanakra clay powder ceramic membrane for water filtration. The fabricated samples could be
 519 sintered to 1300°C to produce porous membranes. They determined the effect of clay powder size on the
 520 membrane efficiency where their membrane was found adequate for membrane filtration at an
 521 inexpensive price using clay, with acceptable efficiency and functionality.

522 It is worth noting the increasing research activities to fabricate separation membranes by 3D printing with
523 the resolution limit and the applicable material being two hindrances that negate its full exploration. As
524 illustrated in **Fig. 5**, the resolution limit of most commercial 3D printers are not high enough to accurately
525 print the pore sizes and tolerances needed. Though some 3D printers such as two photon polymerization
526 (TPP) process can print sub-micron resolution, they are still limited to their printing consistency and
527 tolerance/surface finish, i.e., the prepared model cannot be printed precisely as designed. Also many
528 membranes require far smaller pore sizes such as those for ultrafiltration, nanofiltration and reverse
529 osmosis (non-porous). Due to this limitation, perhaps the approach should be to explore more of the
530 composite membrane designs, rather than to directly print the entire membrane. Another is to ensure good
531 compatibility of the active layer and the support layer materials, preventing any delamination. Until such
532 time that higher resolution capability (i.e., up to nanometer level) can be produced by newer and better
533 3D printers, the direct printing of membranes will remain a challenge. The limitation on applicable printing
534 materials is also negating the direct use of 3D printers for membrane fabrication.

535 **3.3. Photocatalytic material**

536 Heterogeneous photocatalysis works by oxidizing the polluting compounds through the reaction of a
537 semiconductor material that is activated upon exposure of a light source at specific wavelengths [78]. The
538 use of photocatalytic materials such as titanium dioxide (TiO_2) can dramatically increase the rate of water
539 and wastewater treatment. When exposed to light, the catalyst absorbs photon with a larger bandgap,
540 then the formed electron-hole pair allows the catalyst to react with water and dissolved oxygen to generate
541 hydroxyl radicals (OH) and oxide radicals (O_2^-) [79]. In many cases, the material needs to be immobilized on
542 a substrate in order to prevent secondary pollution from the catalysts themselves, and to enable re-use of
543 such photocatalysts. One major issue in conventional photocatalyst substrate is the smaller surface area.
544 Other newer substrates now offer enhanced surface area for photocatalyst immobilization but could pose
545 challenges in synthesis or in making catalytic materials strongly adhered on the substrate. This can
546 potentially be addressed by proper design and fabrication of substrate materials via 3D printing. The main
547 advantage of 3D printing is its capability to finely tune the structure of the target photocatalytic material.
548

549 Due to very high porosity, specific surface area, and self-supported structures of 3D printed photocatalytic
550 materials, they can be exposed to sunlight enabling efficient solar spectrum absorption. Andrey et al. used
551 stereolithography-based 3D printing to pattern the synthesized titanium-rich photoresist using a layer-by-
552 layer approach with 25 μm layer thickness [80]. Structures with different geometries were printed, with UV
553 exposure of the first layer for 14.0 s, four consequent layers for 9.0 s, and all remaining layers for 3.5 s. The
554 process involved pyrolyzing at 1000 $^\circ\text{C}$ under an inert Ar atmosphere, a cubic and octet titania lattice
555 structures with 0.65-1.50 mm unit cells, 115-170 μm beam diameters, and 11-31 relative densities. The
556 SEM results showed beams and unit cells with uniform sizes and a visible layer-to-layer transition patterns.
557 The surface of the structure is uniformly covered by porous nanocrystalline and crystals size ranging from
558 20 to 150 nm. In comparison to titanium foam, the 3D printed part exhibited more strength. Furthermore,
559 the as-designed photocatalytic structure enabled solar water disinfection via the porous structure without
560 using an additional filter. Sangiorgi et. al reported the 3D FDM printing for the preparation of TiO_2
561 nanoparticles utilizing PLA as environmental friendly biopolymers. The structured materials showed 100 %
562 methylene blue (MB) degradation after exposure to light for 24 hours [81]. Vidales et al. reported the AM
563 of titania via depositing TiO_2 in low-density-polyethylene (LDPE) as floated photocatalyst using FDL [82].
564 The materials were fabricated by two different methods: (a) through mixing LDPE and TiO_2 in a hot-cylinder-
565 mixer, and (b) by dispersing TiO_2 and LDPE using o-xylene or an anionic surfactant as a dispersing agent, in
566 order to enhance the dispersion of TiO_2 in the filament before the extrusion process. They investigated the
567 effect of the surface deposition of the printed materials through printing precursors onto TiO_2 mesh which
568 further improves the catalyst performance toward MB degradation, compared to the conventional plate.
569

570 In photocatalysis, the photocatalytic material has to be exposed to the light at specific wavelength in order
571 to maximize its photocatalytic performance. Thus, it is important that this aspect should be considered in
572 the design of substrate material. 3D printing enables production even for very complicated geometries,

573 thus potentially open-cell architecture designs or even those involving fractal designs can be easily
574 fabricated. This open-cell design can allow the light to propagate along the bulk of the photocatalytic
575 material, thus enhancing its overall photocatalytic efficiency. The main challenge with complicated
576 structure is on how to uniformly immobilize the inorganic photocatalytic material on the entire material
577 surface. This can be addressed by preparing a feedstock polymer that has been incorporated with
578 photocatalysts such as titania and then subjecting to pyrolysis to obtain the titania-decorated open-cell
579 structure along the whole surface [83]. Another approach is by impregnation process of photocatalytic
580 material onto a 3D-printed supporting structure [78]. Research by de Rancourt de Mimerand et al. [84]
581 reported the preparation of a very complicated fractal-based 3D-printed (by FDM) structure that was
582 plasma-activated to produce a hybrid photocatalyst fractal structures in the form of fractal pyramids
583 (fracmids). The lamellar fracmids are ideal for photocatalysis as the structure is oriented to capture light
584 efficiently, as proven by the positive outcome of their photocatalytic test results.

585
586 Though 3D printing offers exciting possibilities as an approach to fabricate photocatalytic materials with
587 various designs, however, it does not come without any challenges. For 3D printing, polymers are most
588 commonly used but they suffer from relatively low surface areas, varying thermal stability, and poor surface
589 properties, making them not suitable for direct use in photocatalysis. Thus, in many cases, 3D-printed
590 polymers are used to prepare the substrate for which inorganic photocatalytic nanoparticles are
591 immobilized. For example, not all 3D printing methods and materials are suitable for catalytic applications.
592 FDM mostly uses thermoplastic polymers such as ABS that have low glass transition temperature and low
593 surface area [85], which make them unsuitable for photocatalytic applications as their properties may be
594 affected by the application of heat and light. Increasing the activities of the material may help by
595 incorporating inorganic particles in the polymer filament, but this can also suffer from potential polymer
596 encapsulation of these nanoparticles, which can decrease their performance. To ensure exposure of highly
597 active particles, one approach is to load them directly on the 3D printed material surface, however,
598 delamination becomes an issue. Therefore, ensuring that the active material and the surface have strong
599 interaction is a requisite. SLA printing also has a drawback in that it can only process photosensitive
600 materials, which obviously is problematic for use in photocatalysis.

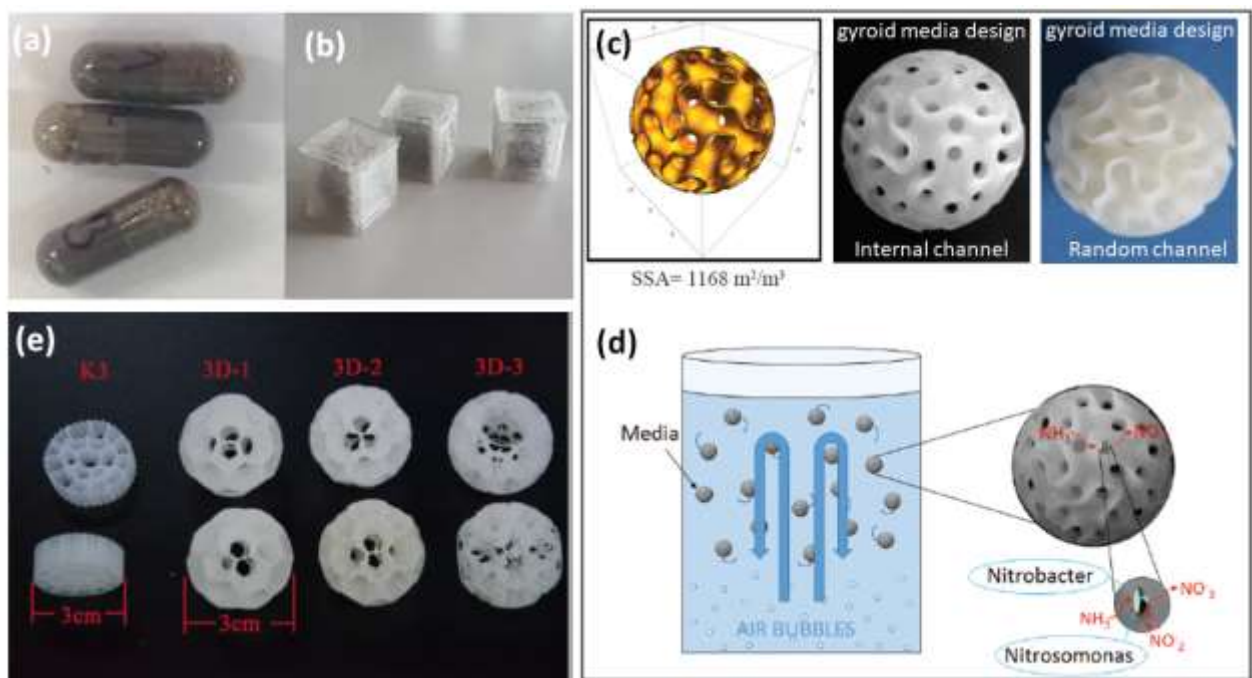
601

602 **3.4. Capsules/bio-carriers for wastewater treatment**

603 Wastewater streams are significant sources of microorganisms, pharmaceuticals, and various compounds
604 that are difficult to be removed by conventional wastewater treatment systems. Post-treatment processes
605 are usually needed to further treat the wastewater effluent. One of the effective ways to breaking down
606 these compounds is through chemical oxidation. Chemical oxidation using ferrate(VI) has shown good
607 efficiency in oxidizing organic and inorganic compounds [86]. However, ferrate(VI) is relatively expensive
608 to produce and is highly unstable in humid environment. By simple encapsulation, ferrate(VI) can be made
609 more stable and its release can be controlled, making it resilient and cost-effective. The capsulation and
610 controlled-release strategy has been reported to be efficient in removing dissolved contaminants in water
611 [87]. With this premise, Czolderova et al. [52] utilized 3D printing to prepare polyvinyl alcohol (PVA)
612 capsules to encapsulate ferrate(VI) (**Fig. 9b**) and were compared with conventionally-made commercial
613 capsules (**Fig. 9a**). Their results indicated long-term storage potential (more than one month without loss
614 of efficiency) of their 3D-printed capsulated ferrate. The degradation efficiency however gave mixed
615 results, achieving more than 80% to most of the micropollutants, but only achieved partial oxidation to
616 others using real wastewater samples. The encapsulation approach using 3D printing in this study could
617 potentially be used to store or apply ferrate in times of emergency. One limitation of the present approach
618 is the multi-step process involving 3D printing of capsule and then loading of ferrate into the capsule. A
619 potential strategy in the future may be a one-step approach of directly printing the capsule with ferrate, or
620 in the form of an open or close construct (such as tablet type) with highly detailed structure to enable
621 tuning of chemical release profiles. This can be made possible by multi-material printers such as those
622 parts printed using polyjet technology.

623

624 Moving bed biofilm reactors (MBBRs) are widely used worldwide for wastewater treatment due to their
 625 simplicity and potential efficiency, allowing attached and suspended growth systems [88]. A lightweight
 626 with high-surface area-to-volume ratio carrier media is highly suitable for MBBR. The performance of the
 627 bio-carrier media highly depends on the formation of biofilms on its surface with good stability. The biofilm
 628 formation is affected by the operating conditions (hydrodynamic, nutrients and oxygen) and the bio-carrier
 629 design (i.e., physicochemical properties such as kind of material, surface properties and texture, pore
 630 spacing, and geometry) providing the growth environment, which affect the overall performance of MBBR.
 631 Having a good bio-carrier design would ensure that bacteria adheres to the maximum area possible, with
 632 good exposure to food and nutrients for survival and growth. Many carrier media with different designs
 633 are available commercially, and most of them are made with simple structures for ease of manufacture
 634 using conventional processes. Improvements in MBBR performance could potentially be achieved if more
 635 complex carrier media structures can be made to increase microbial stimulation and growth. 3D printing
 636 can design and produce complicated designs, thus it can potentially make the most ideal condition and
 637 design for bacterial growth. Elliot et al. [54] prepared a spherical gyroid-shaped carrier media via polyjet
 638 3D printing (see Fig. 9c) and used in MBBR (schematic is given in Fig. 9d). They optimized their design by
 639 modelling and designing a 3D printed carrier with specific surface area (SSA) of up to more than 2300
 640 m^2/m^3 . Wastewater from fisheries was used for inoculation and the results indicated that their 3D printed
 641 gyroid media has comparable NH_3 removal when compared with the baseline K1 Kaldnes commercial media
 642 carrier. However, the exact mechanism of how the 3D printed media stimulates microbial assemblages and
 643 metabolism to affect reactor performance was not elucidated and is ought to be further investigated.



644
 645 **Figure 9.** Chemical oxidation as post-treatment to break down compounds using encapsulated ferrates (a)
 646 commercial conventionally-prepared gelatin capsules, (b) 3D-printed polyvinyl alcohol (PVA) capsules [52];
 647 (c) Different designs of fullerene-type 3D-printed nylon bio-carriers for wastewater treatment using
 648 sequencing biofilm batch reactor [53]; (d) various gyroid media designs fabricated by 3D printing (computer
 649 model, internal channel design, and random channel orientation design for moving bed bioreactor (MBBR)
 650 application. Schematic of the MBBR system is shown in (d) [54].

651 In another study, Dong et al. [53] designed and fabricated novel fullerene-design type bio-carriers using 3D
 652 printing. They intended their new bio-carriers made of nylon (with three designs – see Fig. 9e) to have
 653 specialized structures in order to improve its organic matter removal and overall performance in biofilm
 654 reactors. The physicochemical properties and biofilm growth performance of their bio-carrier was
 655 compared with a commercial K3 bio-carrier made of polyethylene (Fig. 9e). Results indicated greater
 656 surface roughness for their 3DP bio-carriers compared to K3 yet possess much better hydrophilicity. The

657 better surface properties and the specialized hollow design resulted to higher microbial activity (8.73-
658 27.60% higher than K3) and adhesion ability of their 3DP bio-carrier. Compared with fixed bio-carriers, the
659 suspended bio-carriers are designed to move freely in the bioreactor under exposure to flowing water and
660 air. This free motion improves the mass transfer process but can also lead to more collision of bio-carriers
661 hereby causing friction and shearing between them, ultimately leading to slow biofilm formation. On the
662 other hand, fixed bio-carriers can provide higher filling ratio in the bioreactor as they can be arranged
663 homogeneously before operation. To address the limitations of both configurations, Tang et al. [89, 90]
664 designed a semi-suspended spindle-shape bio-carrier media via 3D printing process in order to enjoy the
665 potential high bio-carrier filling ratio in the bioreactor while also providing a restricted freedom of bio-
666 carrier motion. The complexity of the spindle-shape bio-carrier design and structure makes it challenging
667 to fabricate by conventional molding method, thus 3D printing comes into play. Results indicated good
668 growth of diverse microbial community on the 3D-printed semi-suspended bio-carriers.

669 The sizes and resolutions needed to 3D-print capsules and bio-carriers for wastewater treatment are well
670 within the capability of current 3D printers, thus making it as an attractive new option for preparing such
671 materials. In addition, 3D printing can easily manufacture any complex design and structures, giving more
672 leeway to test and prototype bio-carriers with increased surface area, and design that can stimulate new
673 and diverse microbial community. This is in contrast with commercial bio-carriers where they are usually
674 just based on simple patterned structures due to restrictions in conventional manufacturing processes such
675 as polymer extrusion, injection molding, etc. Most of the recent studies on 3D printed bio-carriers have
676 been mainly focused on developing new designs and shapes, and increasing the overall surface area. Future
677 opportunities would be to investigate various surface texture, unique topology designs that provide robust
678 features and dead zones that are essential for anaerobic growth of bacteria. 3D printing could potentially
679 fabricate a novel carrier design involving heterogeneous flow environments (e.g., combined
680 nitrification/de-nitrification process). There is no doubt that 3D printing will play a major role in the
681 production of new generation bio-carriers/filter or capsules in the future.

682

683 **3.5. Sorbents/substrates for oil-water separation**

684 Oil spillage and pollution is one of the main environmental concerns during oil exploitation, extraction, and
685 oil transportation. Oil-water separation technology has been gaining significant attention to address oil
686 clean-up during times of oil spillage and oily discharges [91]. Among the many materials and methods used
687 for oil clean-up, porous membrane structures as sorbents are showing great promise due to their high
688 separation efficiency and recyclability. The porous material allows the oil to pass through the pores but
689 inhibits the water at its surface. This is due to its special wettability (superhydrophobic-superhydrophilic)
690 and high surface-area-to-volume ratio. However, conventional fabrication methods are time consuming
691 and often involve complicated steps. 3D printing has been proposed as a facile way to prototype and
692 fabricate near-ideal porous membrane structures with desirable properties for oil-water separation.
693 Studies utilizing both polymeric and ceramic-based materials have been reported in recent years for oil-
694 water separation.

695 The challenge of coating superhydrophobic structures at a micro/nano level on the surface of a substrate
696 for oil-separation has driven Lv et al. [63] to use 3D printing technology. In their study, polydimethylsiloxane
697 (PDMS) ink containing hydrophobic nanosilica was coated on a mesh structure by 3D printing. The presence
698 of the nanosilica in the ink imparted good printability and provided mechanical strength on the coated
699 material. Topographical structures to provide superhydrophobicity was controlled. A very high flux of
700 23,700 LMH was achieved and a water-oil separation efficiency of 99.6% at a pore size of 0.37 mm. Shin et
701 al. [92] on the other hand got inspiration from nature (cactus plant) and prepared a bio-inspired PDMS
702 sponge. A 3D printed mold served as template to fabricate the PDMS sponge. The sponge has a hollow,
703 porous structure at the center that serves as the oil storage space. Results indicated the effect of surface
704 pore size and line width on the absorption capacity, wherein the bigger pore size and decreasing line width
705 lead to increasing capacity. The present bio-inspired PDMS sponge showed almost 4 orders of magnitude
706 increase in absorption capacity compared to conventional PDMS sponge. Another study [93] prepared a

707 bio-inspired (based on lotus leaf) 3D-printed (FDM technology) superhydrophobic poly(lactic acid) or PLA
708 packings. A high oil-water separation of 95% and relatively high flux were achieved. Yuan et al. [49] used
709 selective layer sintering method of 3D printing to prepare polysulfone membranes for oil-water separation.
710 To impart increased hydrophobicity, the 3D-printed polysulfone membrane was surface-coated with candle
711 soot by immersion, which resulted into a Janus-type membrane. The candle-soot treated membrane
712 surface was superhydrophobic (161° water contact angle, and 5° water sliding angle), while the bottom
713 (untreated) surface, was hydrophilic. Oil-water separation efficiency was maintained at 99% even after 10
714 cycles.

715 Most of the oil-water separation materials are polymer-based, thus when they are exposed to harsh
716 conditions, they can degrade and lose their efficiency. In this situation, a ceramic-based material would be
717 ideal. This inspired Chen et al. [62] to develop a 3D-printed ceramic-based (alumina) water-oil separation
718 material functionalized on the surface with aluminium borate whiskers. The oil-water separation efficiency
719 was >99% while maintaining high flowrate. Most interestingly, the prepared material showed high oil-water
720 separation performance and durability even when exposed to harsh environments such as those solutions
721 containing organic solvents, at high temperature and highly acidic condition. Their material showed better
722 durability than metal or polymer-based counterparts. The final 3D printed material was easily optimized by
723 simple high temperature heat treatment.

724 There has been increasing number of research using 3D printing to prepare sorbent materials for oil-water
725 separation especially in the past three years. Aside from the rapid prototyping ability, 3D printing can also
726 allow control of inner structure and surface, which definitely adds huge benefits for the sorbent's overall
727 performance. This goes to show the promising approach to fabricate sorbent materials with user-defined
728 and functional features. This include control of surface structure (e.g. roughness) that can generate
729 superhydrophobic surface or oleophilic surface, though still limited on the printer resolution limits. Just like
730 for a filter, the pore sizes or porosity needs of the sorbent materials may be a challenge for 3D printing if
731 precision is needed going below one micron range. The kind of materials for 3D printing is still also rather
732 limited especially for the specific properties needed for oil-water separation. In many cases, surface
733 modification is still necessary in order to produce the desired surface characteristics. Polymers are still
734 mostly used over ceramic ones especially as sorbents. Physical sorbents need some form of flexibility, in
735 which polymeric materials can provide; though 3D-printed ceramic structure in the form of filter may be
736 more advantageous in highly challenging environments. Another important aspect to consider for 3D-
737 printed materials is the mechanical integrity of the sorption material. This also pertains to the robustness
738 of interfacial bonding between the 3D printed material and the coating layer or nanoparticle inclusions as
739 the sorbent will be subjected to challenging environments (highly acidic or alkaline) and various loadings
740 (e.g., bending, squeezing for regeneration, etc.). As indicated in a previous study [18], the intrinsic property
741 of the feedstock material before printing greatly affects the resulting mechanical property of the 3D-printed
742 structure. In addition, the 3D-printing method and the build orientation are also two important factors on
743 the resulting mechanical properties. An interesting direction for sorbent materials maybe towards smart
744 sorbents via 4D printing, where multi-functionalities are provided on the sorbent as activated by an
745 external stimuli such as pH, temperature, etc.

746

747 **3.6. Solar absorbers for solar steam evaporation**

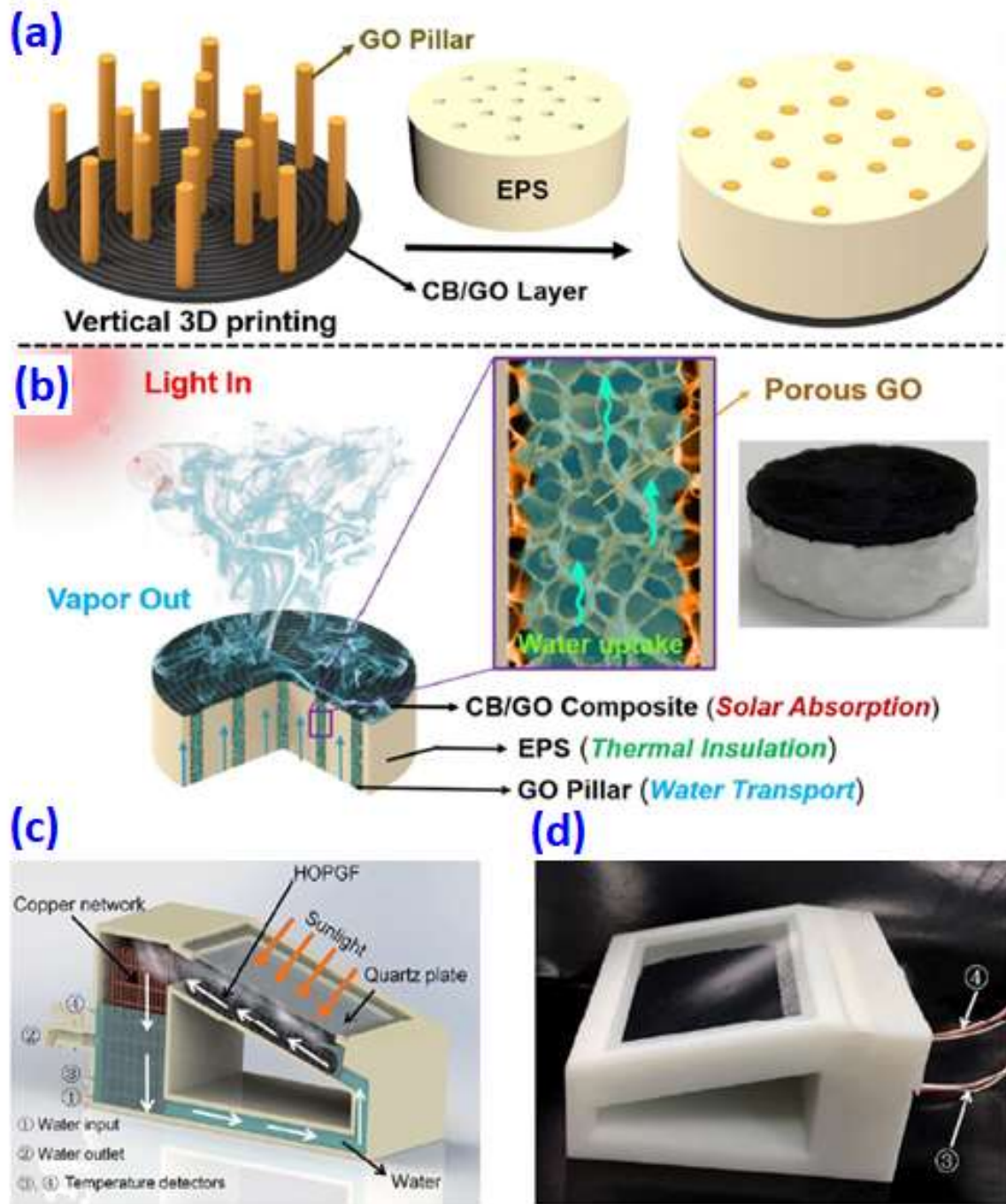
748 Solar-driven water evaporation through utilizing solar illumination projected to photothermal materials has
749 attracted tremendous attention in recent years as a potential solution for the shortage of clean water [94].
750 A good photothermal material for high efficiency solar steam evaporation (SSE) should possess the
751 following: a broad light absorption over near infrared region (NIR), low thermal conductivity and a
752 hydrophilic surface with open porous structures [95, 96]. In the past ten years, SSEs containing noble metals
753 (e.g., Au, anodized aluminium oxide) and carbon materials (carbon nanotube (CNT) and graphene oxide
754 (GO) e.g.) have been widely investigated. However, the main challenge for the technology is to fabricate
755 easy-to-manufacture and scalable approaches, which can convert solar illumination into useable thermal
756 energy with high energy efficiency. To address this challenge, researchers applied 3D printing technologies,

757 enabling the prototyping and fabrication of photothermal materials with designed architecture and
758 patterns for SSE applications with high energy efficiency. Vertical printing-based [97] and extrusion/direct
759 ink writing-based [96] 3D printing techniques, appeared to be the most promising techniques for the design
760 of 3D engineered materials with excellent properties and multi-functionalities for SSE. For instance, Yiju et
761 al. [55] fabricated and designed a 3D-printed all-in-one evaporator with a concave structure that possessed
762 a high porosity of 97.3% and an efficient solar absorption (>97%). The integrated SSE structure consisted of
763 CNT/GO layer, GO/nanofibrillated cellulose layer (NFC), and GO/NFC wall. The as-designed materials
764 achieved a solar steam generation efficiency of 85.6% under 1 Sun irradiation (1 kW m^{-2}), and obtained an
765 evaporation rate of $1.25 \text{ kg m}^{-2} \text{ h}^{-1}$. The authors attributed the performance to the low intrinsic thermal
766 conductivity of porous evaporators, which facilitated heat localization and effectively minimized thermal
767 dissipation to the bulk water.

768
769 In another study, 3D vertically-designed jellyfish-like evaporator was designed and fabricated by a vertical
770 3D printing technique [56]. It was prepared by printing a GO pillar vertically on a porous carbon black/GO
771 layer (porosity~93%) (**Figure 10a**). The open porous structure of the evaporator absorbs high light within a
772 wide optical absorption (250-2500 nm). In addition, the uniform distributed GO pillars was expected to
773 decrease the horizontal water transport path length resulting in a sufficient water supply for steam
774 generation. Furthermore, as described in **Figure 10b**, direct water pathways can significantly minimize the
775 contact area between the illumination layer and bulk water, which can in turn prevent heat loss to the bulk
776 water and further enhance steam generation efficiency. The addition of expanded polystyrene (EPS) foam
777 thermal insulator plays a significant role in suppressing heat dissipation to the bulk water. Therefore, the
778 solar steam device showed an efficiency of 87.5% under 1-sun illumination. The ion concentration of Na^+ ,
779 K^+ , Mg^{2+} and Ca^{2+} of the seawater after purification were found to be far below the World Health
780 Organisation (WHO) standards for drinking water.

781
782 He et al. fabricated freestanding 2D carbon nitride hybrid aerogel membrane with patterned macroscopic
783 architecture using 3D printing [57]. The ink was prepared by mixing gold (Au) nanobipyramids, $g\text{-C}_3\text{N}_4$
784 nanosheets (Au/CNNS) dispersion and sodium alginate (SA) solution to increase the viscosity and obtain an
785 optimum rheological behaviour for the smooth extrusion from a fine nozzle. Later on, the ink was printed
786 on air, or into a reservoir of a CaCl_2 /glycerol solution, or Pluronic F127. The as-printed structure exhibited
787 broadband absorption in near infrared region (NIR) and an excellent solar light absorption. The as-obtained
788 result was 2.5 times that of the baseline sample, which is attributed to the solution diffusion efficiency and
789 liquid velocity of the 3D printed structure. Graphene inks are extensively studied for printed flexible
790 electronics, because of their extraordinary high electronic conductivity and mechanical flexibility, as well
791 as their chemical stability [98-101]. For example, Zhang et al, designed a 3D solar water heater housing self-
792 supply model using 3D printing, composed of highly vertically ordered pillar arrays of graphene-assembled
793 frameworks (HOPGF) (**Figure 10c and 10d**) [102]. It could potentially heat 30 Kg of water up to $50 \text{ }^\circ\text{C}$ with
794 only one square meter of HOPGF under 1 sun within hours. They further demonstrated its practical
795 application in a building with a roof area of 100 m^2 , where large amount (480 kg) of water per day could be
796 produced. This designed structure provided an efficient material for solar driven water treatment for
797 practical applications. However, the cost of the materials is a main challenge and alternative low-cost
798 carbon sources should be considered.

799



800
801
802
803
804
805
806
807

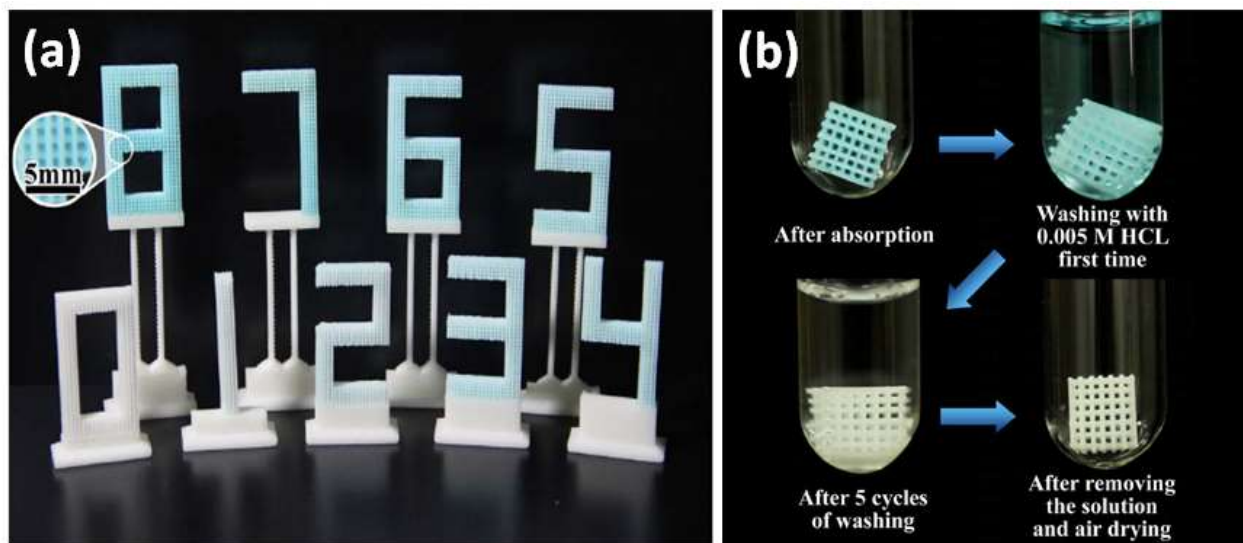
Figure 10. (a) Schematic describing the vertically-oriented 3D printed evaporator which is inserted in EPS foam; (b) principle illustration of the 3D printed evaporator and its corresponding photographic image [97]; (c) schematic illustration of the designed solar water heater system and (d) its corresponding photographic image [102].

3.7. Adsorbents/substrates for dye degradation

808
809
810
811
812
813

Carbon based materials are widely used as adsorbents for organic dye removal, however, the process of separation and recycling is intrinsically complicated. This is because the materials are in powder form thus have a lack of flexibility [103, 104]. The 3D printing process provides flexible materials with porous and open structures that can directly adsorb organic dyes with high efficiency, and can potentially be recycled. One of the promising materials for many different applications is metal organic frameworks (MOFs), which possess porous crystalline structures, open channels and large surface areas, composed of several

814 functional groups [58, 105]. These inherent features provide a promising material with wide applications
815 such as the removal of organic dyes. To enhance the flexibility of MOF, Wang et al. utilized 3D printing for
816 the fabrication of acrylonitrile butadiene styrene (ABS) coated with porous Cu-Benzene tricarboxylic acid
817 adsorbents for methylene blue (MB) removal [58]. The preparation process involves the coating of Cu-BTA
818 onto a 3D printed ABS surface. The Cu-BTC/ABS composite enhances surface wettability, which in turn helps
819 to enhance the adsorption of metals and linkers. The composite was designed in a variety of number shapes
820 (Figure 11a). The SEM images reveal that the printed composite exhibited a smooth surface with some
821 small hills. MB removal efficiency of 93.3% and 98.3%, for solution with concentrations of 10 and 5 mg/L,
822 respectively, was achieved within 10 min. Figure 11b illustrates that the composite could be recycled
823 without any complications displaying its promising practical application.
824



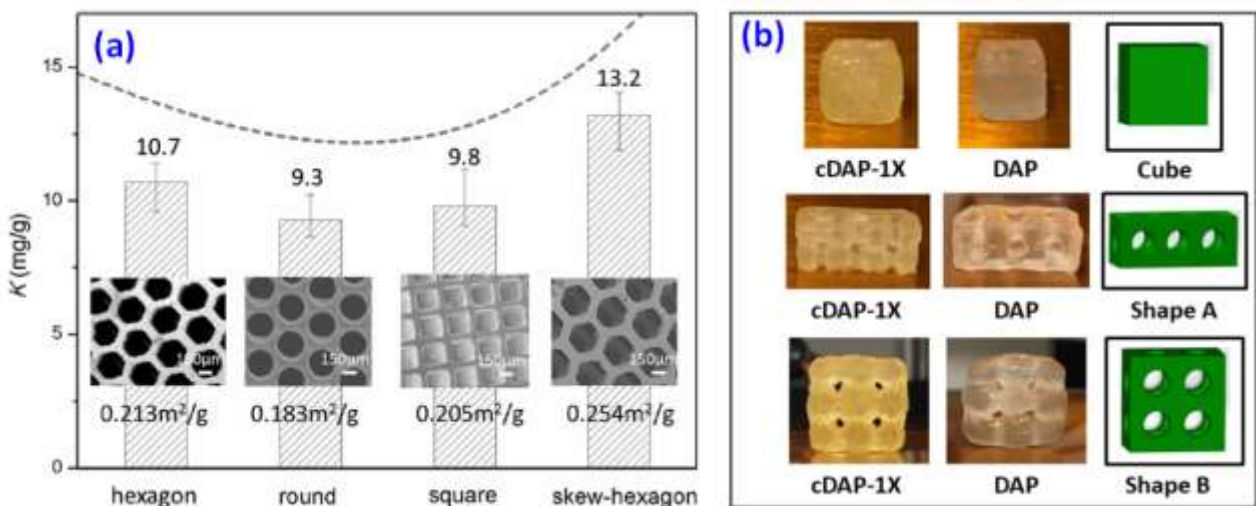
825
826 **Figure 11.** (a) Photographs of the synthesized Cu-BTC/ABS composites (the printed number illustrates the
827 number of cycles); (b) Photos of the recycling process of ABS polymer skeleton. (adapted from [58]).
828

829 In contrast, Figuerola and his co-workers incorporated sub-micrometric crystals of a Zeolitic Imidazole
830 Framework (ZIF-67)/ polymer mixed matrix on 3D printed device through a sample coating process [59]. The
831 device was used for the degradation of Rhodamine B as a model dye. The 3D-coated device exhibited an
832 average degradation of 97-98% after 10 cycles with excellent reproducibility and reusability. Liu et al. used
833 a direct ink writing (DIW) 3D printing to fabricate nitrogen-doped carbon materials with different
834 mesopores/micropores and monolithic structures with surface area of $816 \text{ m}^2\text{g}^{-1}$. The ink was prepared by
835 adding melamine, which acts as a nitrogen source to the starch gelatin system, and SiO_2 as a template.
836 Freeze-drying and carbonization steps were done after 3D printing, while the template was removed via
837 etching method. The printed monolithic structures showed an excellent adsorption of MB dyes. Further,
838 the materials can be recycled without any complicated process.
839

840 Adsorbent materials or substrates for dye degradation need high surface area to enhance the adsorption
841 sites and efficiency. Moreover, for practical application, mechanical stability for cyclic use of the adsorbent
842 is an important requirement. In many cases, adsorbent materials are changed by modifiers (bio-based or
843 inorganic modifiers such as CNTs, clay, etc.) by mixing or coating. However, there is high possibility of poor
844 adhesion of coating layer or modifiers to the 3D-printed substrate, which could thereby lead to
845 delamination and potentially cause secondary pollution. Challenge still remains on the ability of the current
846 3D printer to follow the exact CAD model at the highest resolution, i.e., achieving the micro to nano-level
847 roughness which supposedly can increase the surface area is still unachievable. Efforts in the future should
848 focus on enhancing the adhesion between fillers and polymer matrix, and improving the current print-head
849 designs of 3D printers (e.g., FDM) that would allow less or no pre-processing or mixing.
850

851 3.8. Adsorbents for heavy metal adsorption

852 The removal of heavy metals from water including copper, lead, cadmium and mercury has received
 853 considerable attention due to their toxicity. These toxic metals have severe detrimental effects on human
 854 health via accumulation through the living organism [106, 107]. Therefore, a scalable and sufficient method
 855 to remove these toxic metals is essential for the safety of the public. Adsorbents such as activated carbon,
 856 carbon nanotubes, bio-inspired materials, and other porous carbon materials have been proposed for the
 857 removal of heavy metals through a porous media. Prominent is the use of bio-inspired materials, due to its
 858 intrinsic advantages of low-cost, effectiveness and biodegradability [108, 109]. Chitosan is an example of a
 859 biocompatible material, which can adsorb heavy metals, but it suffers from poor reusability and
 860 processability. 3D printing overcomes the issues through designing 3D structures that possess a porous
 861 structure and a large surface area, as well as potential reusability. For instance, Zhang et al. designed bio-
 862 adsorbents consisting of monolithic 3D porous chitosan composite adsorbing filter via stereolithography-
 863 based 3D printing technique and applied it for Cu removal [108]. Several structures were designed such as
 864 closely arranged hexagonal holes, round holes, square holes and skewed hexagonal holes. **Figure 12a**
 865 reveals the composite with skewed hexagonal holes and emerged as the most efficient structure with a
 866 high adsorption. The reusability was investigated by an adsorption-desorption test with an aqueous
 867 ethylenediaminetetraacetic acid (EDTA) solution as the eluent. Around 92% desorption capacity was
 868 achieved and the value remained constant throughout the process proving its reusability. The authors only
 869 limited the applications to Cu(II) removal. The application of 3D printing was further expanded to generate
 870 materials with a unique structure. For instance, hydrogel materials (**Figure 12b**) were considered as heavy
 871 metal adsorbents, because of its advantages of having open porous structure with a large surface area. For
 872 example, extrusion based 3D printing was applied to fabricate 3D hydrogel structures for heavy metal ion
 873 removal (Cu^{2+} , Pb^{2+} , Cd^{2+} , Hg^{2+})[109]. The hydrogel was prepared by mixing chitosan and diacrylated Puroic
 874 F-127 (F127-DA) at different ratios. The results showed that the printability of chitosan reduced as the
 875 concentration of chitosan increased. The hydrogel with structural features adsorbed up to 95% of metals
 876 within 30 min.
 877



878
 879 **Figure 12.** (a) Comparative illustration of the adsorption capacity for Cu(II) of chitosan-based 3D-printed
 880 filters with varying designs ($T=25\text{ }^\circ\text{C}$, $\text{pH } 5.5$) [108]; (b) 3D-printed hydrogels used for removal of different
 881 heavy metals (Cu^{2+} , Pb^{2+} , Cd^{2+} , Hg^{2+}) [109].
 882
 883

884 For heavy metal removal, 3D printing provides an exciting avenue to create materials in various forms and
 885 shapes with ease of preparation, may it be as hydrogels, filters, sorbents, etc. regardless of the complexity
 886 of the design. The specific surface area is an important parameter for adsorption processes, thus enabling
 887 precise design and manufacture of internal structure by 3D printing definitely is an advantage for such an
 888 application. 3D printing is also an approach for a “greener” fabrication of chitosan-based adsorbent
 889 membranes for heavy metal removal. Instead of using large amounts of solvents and acids/bases to process
 890 chitosan, a facile way is to directly 3D-print (by SLS) chitosan mixed with thermoplastic polyurethane (TPU)

891 for a solvent-less membrane fabrication method [110]. Cu(II) and Pb(II) were efficiently adsorbed on the
892 membrane. In recent years, chitosan-based hydrogels have been increasingly investigated using 3D-printing
893 due to the ability of hydrogel to respond quickly with external stimuli with reversible volume changes (this
894 is essentially 4D printing). 3D printing can either be used to directly print the sorbent material, print the
895 substrate for which it is functionalized with sorptive properties, and print the template for which sorbent
896 material is molded. All these approaches provide precision-3D-printing of any geometrical shapes and
897 structures that are otherwise very difficult to achieve by conventional fabrication technique. Making
898 composite 3D-printed material decorated with heavy-metal binding sites is also a good strategy, but issues
899 on defects due to nanofiller content especially when using thermoplastic polymers are a concern [105]. The
900 nanofillers can induce void formation thereby affecting the overall mechanical integrity of the 3D-printed
901 structure.

902

903 4. Challenges of 3D printing

904 4.1. Material and process limitations

- 905 a. **Resolution/accuracy** - Limited resolution or layer height: This limitation is a particular disadvantage for
906 the direct fabrication of membranes, where layer height and pore sizes of most membranes are in the
907 sub-micrometer level. The further development of the two-photon polymerization which could print
908 to a very high resolution of ~100 nanometers would potentially be able to address this issue [111].
909 Many of the available 3D printers and 3D printing technologies today have issues regarding
910 accuracy/precision of printed parts in comparison with the 3D model, and needs to be redesigned and
911 reprinted for a more accurate part (i.e. perfect fit).
912
- 913 b. **Limited types of applicable 3D printing materials available/performance-** Adding more types of 3D
914 printing materials is needed (especially those being used for conventional membrane production such
915 as polyvinylidene fluoride (PVDF), polypropylene, polytetrafluoroethylene (PTFE), polyimide,
916 polyamide, polyethersulfone, polyetherimides, etc; simultaneous printing of multiple materials having
917 different properties and functions would also advance the adoption of 3D printing technologies for
918 membrane design and fabrication. The material used and the 3D printing technique also dictate the
919 resulting properties and performance of the 3D-printed part. Mechanical strength is an important
920 parameter and 3D-printed materials should be able to withstand high amounts of pressure under
921 various challenging environments. This is especially true when dealing with wastewater or saline water
922 where the pH level may be extreme or there are various impurities in the solution. There are certain
923 types of polymers (e.g. photopolymers) that undergo swelling when soaked in water due to its
924 hydrophilic behavior [112]. In some materials, this could affect the structural integrity of the printed
925 part. Proper selection of photopolymer and photoinitiator is crucial when using the SLA-AM technology.
926 Also, in some cases, the solution may degrade (especially) the polymer materials.
927
- 928 c. **Slow printing speed / Poor scalability / Need for post-processing-** 3D printing is a highly customizable
929 but slow process. Printing a large piece with high resolution could take a very long time to finish. New
930 3D printing technologies such as the CLIP process could potentially solve this issue [113]. Limited build
931 size: 3D printers should be able to print at least 1 meter in width to enable fast production and upscaling
932 especially if preparing membranes. The staircase effect is an example of an inherent characteristic of
933 3D-printed parts which needs post-processing. SLS - AM produces rough surfaces, which could either
934 be advantageous or disadvantageous to membrane design especially on its effect on the
935 fouling/antifouling properties [114].
936
- 937 d. **Cost-** 3D printing is still relatively more expensive than many other conventional and formative
938 fabrication techniques due to material requirement and fabrication times, and most especially when
939 compared to conventional membrane fabrication techniques. For example, for FDM printing using ABS
940 material (commercial-grade), it can cost around US\$250 per kilogram, or for stereolithography, >US\$200

941 per kilogram for photopolymers [13]. This does not take into account the lost or unused material after
942 printing. There is a need to significantly reduce the cost of printing materials, technologies and
943 processes (e.g. laser-based technologies consume relatively more power/energy during operation).
944

945 **4.2. Safety and environmental concerns of 3D printing**

946 While it is true that 3D printing has greatly revolutionized the manufacturing technology, there are some
947 environmental impacts and safety concerns that need to be addressed. One of the hazards of 3D printing
948 processes is the particulate emission, such as ultrafine particle emission (UFP) and volatile organic
949 compound (VOC) emission, from the materials being used. According to Azimi et al., UFP emission rate is
950 highest when using ABS and polycarbonate filaments, and lowest at PLA and other filaments such as nylon.
951 The individual VOC emission rate is highest among nylon-based, laywood and laybrick filaments, ABS, and
952 high-impact polystyrene (HIPS) filaments. Until a low-emitting filament is designed to reduce the UFP and
953 VOC concentrations, it was suggested to avoid working on 3D printers in an enclosed space with poor
954 ventilation or without gas and particle filtration system [115].

955 Kim et al. reported that FFF printers emit high concentrations of nano-size particles including carcinogenic
956 formaldehydes, phthalates and some VOCs such as toluene and ethylbenzene [116]. In SLS printing,
957 operators can have significant exposure to polymer or metal particles when handling powders [117].
958 Moreover, solvent baths are sometimes used in FFF and SLS prints in order to remove the supports or to
959 improve the surface quality. For postprocessing of DLP and SLA prints, alcohols or propylene carbonate are
960 used when removing the residual resins [118]. These solvents can be toxic to humans and environment if
961 not properly handled.

962 Studies on life cycle assessment (LCA) were conducted to identify the human health risks and
963 environmental as well as ecological impacts of 3D printing technology from material sourcing and handling
964 to printing process and waste disposal. Faludi et al. concluded that the sustainability of 3D printers depends
965 mainly on the proper utilization of machines to reduce the idling energy and to be more efficient in
966 electricity usage. The energy demand during printing process dominates the environmental impacts of 3D
967 printing technology [119]. The environmental burdens and health hazards can be minimized through these
968 assessments and by optimizing and improving the 3D printing processes.

969

970 **4.3. Industrial upscaling challenges and potential of 3D printing**

971 Additive manufacturing (or 3D printing) is still at its growing stage and still faces many challenges especially
972 for industrial upscaling. However, the tide could potentially change anytime soon with the provision of
973 more powerful and bigger 3D printers, wider range of new feed stock materials, and new way of
974 measurement and product quality control. There is significant interest from industry to adopt the AM
975 technology in their processes, and in fact, AM has already shifted from prototyping to production. Using
976 3D printing, production of parts on demand (i.e. produce-to-order) would enable manufacturers to print
977 parts as needed instead of producing-to-stock. This could significantly reduce inventory and storage costs.
978 Distributed manufacturing, which is the manufacturing of the product closer to customers, is also made
979 possible by 3D printing (which is a form of digital manufacturing). Essentially, 3D CAD files will be sent to
980 smaller sites or remote locations. Also, development of materials for specific applications is very important
981 for industrial applications. Specifically, development of 3D printing materials that are cheaper, stronger,
982 more lightweight, more environment-friendly are important research topics for the adoption of 3D printing
983 for industrial applications. Customization for industrial applications would be vital especially for rapid parts
984 replacement (of hard to find parts) [120]. Currently, 3D printing is more suitable to high value (complex
985 design) low volume products compared with traditional manufacturing wherein economies of scale is an
986 important consideration to recover cost. The adoption of 3D printing to industrial applications at this stage

987 is more geared towards producing parts that are impossible or more expensive if conventional
988 manufacturing is used [121].

989 A number of companies have slowly adopted the use of 3D printing in their processes. For example, Adidas,
990 in partnership with Carbon, printed high quality midsoles for sneakers. Carbon uses high-
991 performance/precision LED light (Digital Light Synthesis Technology) that projects images of the cross-
992 sectional areas of the parts. BMW is using the powder-based selective laser melting (SLM) technology to
993 make mountings for the top cover of the roof mechanism (opening/closing). Rehook, developed by cyclists,
994 is a tool, which helps reattach dropped bike chain back on track. Designers use graphite-filled nylon material
995 and SLS 3D printers. With these examples, it can be said that 3D printing is now getting ready for mass
996 production, however, the cost and complexity of part (design) will play a big role in determining whether
997 to choose traditional way of manufacturing (i.e. subtractive manufacturing and formative manufacturing)
998 or additive manufacturing (i.e. 3D printing) [122]. Serial production, which is one type of mass production,
999 is used in the production of items in series made in the same way. FDM printing is now poised to be used
1000 in serial production due to its cost and ease of production. 3D printing farm, which is a collection of 3D
1001 printers arranged alongside each other can be an approach for mass production of parts, with the objective
1002 of on-demand and efficient manufacturing. However, the initial cost and maintenance will be an issue.
1003 Many companies have recently joined the race in creating large-scale printers (print dimension exceeding
1004 1 m) to offer to the market.

1005 One of the main challenges in adopting 3D printing for industry use is the functionality of the part, which is
1006 very much related to how it is used by the market. An important consideration also is the behavior of the
1007 parts during its use (operation) which is related to its properties (metrology – pertaining to real time quality
1008 measurements), for example mechanical properties when used for structural applications. Of course
1009 ultimately, the cost should be considered [121]. Another important factor is the software used and the
1010 techniques and skills to optimize the use of available computer programs. One issue is on designing the
1011 part including the support and internal structures. Another consideration is the development of user-
1012 friendly software. The goal of software developers is to decrease the expert knowledge needed by users to
1013 3D print. In connection to this, the development of an operating system which could be adopted by all 3D
1014 printer OEMs, similar with the Microsoft Windows Operating System. Generative Design, which is an
1015 iterative design method involving a computer program that generates several outputs meeting certain real-
1016 world constraints, should also be considered [123].

1017 The potential of 3D printing in the future seems to be unlimited if all the challenges are addressed. The
1018 expectation is that there will be more spin-off innovative and exciting applications that will come in the
1019 long term due to more precise 3D printers at lower cost, new materials, and high quality automated control
1020 from pre-processing until post-processing.

1021

1022 **5. Future prospects**

1023 **5.1. Combination of 3D printing + other processes**

1024 A potential future direction of 3D printing may be one that is not entirely a stand-alone process but more
1025 of integrated multi-process system, by its combination with other manufacturing processes. This is
1026 particularly true for membrane fabrication for desalination and membrane separation processes, as the 3D
1027 printing resolution is not yet able to directly print the entire membrane at the resolution needed.
1028 Therefore, a combination of conventional active layer fabrication and 3D printed middle or support layer
1029 would be attractive as already demonstrated by a few recent studies.

1030 **5.1.1. 3D printing + electrospinning/spraying or solution blow spinning**

1031 One way of combining two processes to fabricate a composite membrane is the combination of 3D printing
1032 and electrospinning. This is interesting for membrane preparation for water treatment as the 3D printed
1033 support layer can be designed and fabricated with high porosity, while the active layer can be made from
1034 ultrafine electrospun nanofibers where pore sizes can be easily tailored. This type of nanofiber/3D printed

1035 layer combination has been actively researched in the biomedical field, but not yet in the water treatment
1036 field. For example, Lee et al. [124] combined electrospinning and 3D bioprinting in the preparation of a bio-
1037 tubular scaffold used for the fabrication of artificial vascular graft. Surface morphology and mechanical
1038 properties increased using this hybrid method. Rajzer et al. [125] also combined 3D printing and
1039 electrospinning in creating a multifunctional layered scaffold for subchondral bone reconstruction and
1040 nasal cartilages. The mechanical properties of 3D-printed scaffolds with varying internal architecture were
1041 tested. Naghieh et al developed hierarchical scaffolds using FDM 3D-printed micro struts (using polylactic
1042 acid – PLA) and electrospun nanocomposite fibrous layers (using gelatin-forsterite) and concluded it can be
1043 used for bone tissue regeneration [126]. The main issue with composite membrane approach is the
1044 delamination possibility at the interface layer of the nanofiber and the 3D printed membrane.

1045 In relation to membrane and module preparation, there is a need for validation of different membrane
1046 designs with computational fluid dynamics (CFD) [3]. As accurate simulations of some parameters are not
1047 possible using CFD [44], employing additive manufacturing in rapid prototyping and rapid validation would
1048 be very important. Lee et al [3] added that CFD analyses may be combined with additive manufacturing in
1049 validating complicated geometries. With module casings, feed spacers and other related module parts
1050 having dimensions above the millimeter scale, additive manufacturing is now being adopted for the design
1051 and prototyping of these components.

1052

1053 **5.1.2. Hybrid manufacturing combining additive manufacturing with subtractive manufacturing and** 1054 **formative manufacturing**

1055 There is a potential synergistic effect of hybridizing additive manufacturing with other conventional
1056 manufacturing techniques. The process can start with the 3D printing (additive manufacturing) of injection
1057 molds, and then followed by injection molding (formative manufacturing) of material (e.g. plastic) onto the
1058 mold, and lastly employing subtractive manufacturing (e.g. drilling, milling, etc) to add or enhance some
1059 features, as well as to do finishing/post-processing. Hybrid manufacturing using 3D-printed molds has
1060 several advantages, such as [127]:

- 1061 1) Fast launching: 3D printing of molds usually just takes a few days to conceptualize, and several
1062 hours to print.
- 1063 2) On-demand fabrication: easy correction/redesign of molds is possible.
- 1064 3) Cost-effective production: 3D-printed molds are cheaper than molds fabricated using conventional
1065 mold fabrication.
- 1066 4) Freedom of geometry design: complex designs are easier to build using 3d printing compared with
1067 traditional tooling process.

1068 This could be potentially implemented for bigger parts needed such as modules for solar water evaporation,
1069 membrane modules, and templates for hydrogels for adsorption. This would not be ideal for very thin parts
1070 such as membranes due to inaccuracy concern, thereby relating to product quality as well. Another hybrid
1071 technology is similar with the Large Additive Subtractive Integrated Modular Machine (LASIMM). It has
1072 additive and subtractive manufacturing capabilities. Specifically, it has additive manufacturing, cold-work,
1073 machining, metrology and inspection capabilities [128].

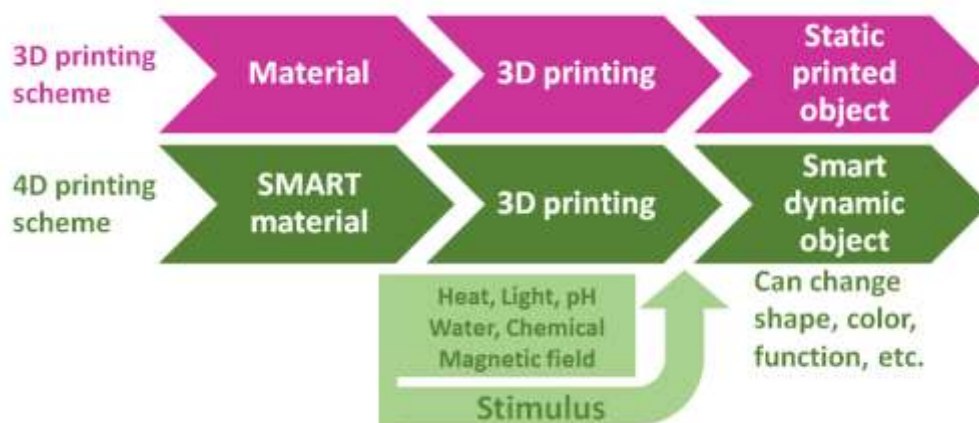
1074

1075 **5.2.4D printing**

1076

1077 Another exciting research direction would be by 4D printing approach to fabricate materials for water-
1078 related applications. 4D printing is an “upgrade” of 3D printing, adding the element of time, i.e., the
1079 property, function or shape of a 3D-printed part can change as a function of time [30] (see differences in
1080 **Fig. 13**). This makes the 3D printed object “alive” by exposure to external stimuli. Examples of such

1081 transformation/shifting include bending, folding, twisting, surface curling, linear or nonlinear expansion,
 1082 and surface generation (e.g., wrinkles, buckles and creases) either from 1D, 2D, 3D structures or their
 1083 combination [129]. With 4D printing, multi-functionality, self-assembly, reconfiguration, replication and
 1084 self-repair is possible. Thus, this provides certain advantages such as reduction of volume for storage, and
 1085 shape transformations which is possible with flat-pack 3D-printed structures. 4D printed structures can see
 1086 major applications in medicine, space, satellites, construction, architecture, sensing and actuation, and in
 1087 membrane separation [129]. Shape-shifting materials are mainly two types, namely, shape-memory
 1088 materials and shape changing materials which are extensively discussed previously [129, 130]. This is
 1089 possible with the right combination of smart (e.g. active expandable polymer) and conventional (e.g. rigid
 1090 plastic) materials [131, 132], stimulus, interaction mechanism, mathematical modelling, as well as with the
 1091 appropriate printing technology. Appropriate materials are usually those which could swell or expand.
 1092 Specifically, characteristics of smart materials include shape memory, responsiveness, and
 1093 multifunctionality among others. Further, previous reports showed different material classifications, for
 1094 example single-material or multimaterial structures; other groups classified the materials as composite
 1095 materials, discrete multiple materials and porous materials [133]. Further, other groups classified under
 1096 digital materials and further categorized as uniform distribution, gradient distribution, and special patterns;
 1097 another one is structures with and without hinges and joints.
 1098



1099
 1100 **Figure 13.** Differences between 3D printing and 4D printing processes and the capability of the printed
 1101 objects. For 4D printed structures, the printed objects come “alive” upon exposure to various stimuli.
 1102 (modified from [129])
 1103

1104 The important consideration for using materials are printability and intelligence. 3D printing technologies
 1105 used include FDM, mask-image-projection-based stereolithography, high resolution
 1106 microstereolithography with automated material exchange mechanism, and direct-write printing, etc.
 1107 Stimuli include heat, light, water or various combinations of all these. Examples of interaction mechanisms
 1108 include constrained thermo-mechanics [134], unconstrained thermo-mechanics [135], unconstrained
 1109 hydro-mechanics [131, 132], unconstrained hydro-thermo-mechanics [136], unconstrained thermo-photo-
 1110 mechanics [137], osmosis-mechanics [138], dissolution mechanics [139], and unconstrained-pH-mechanics
 1111 [140]. Mathematical modelling is needed in order to predict the shape-shifting of the material/s, to reduce
 1112 the number of experiments (trial and error), and to prevent collisions of components during shape-shifting.
 1113 Inputs to mathematical models include the shape, material properties, material structure and stimulus
 1114 properties [129]. Matthews et al. [141] reported the 3D printing of acrylic polymer containing biological
 1115 materials, i.e. membrane proteins using a DLP 3D printer. The fourth dimension is the bio functionality of
 1116 these proteins. The authors reported on the 4D printing of a bio-inspired nano hybrid electrode for water-
 1117 splitting applications. They use a polymeric resin with proton-pumping bacteriorhodopsin (bR), carbon
 1118 nanotubes (CNT), and silver nanoparticles (Ag NP). The authors claimed that “these printed photo
 1119 electrochemical cells exhibit high durability, low onset over potential, and upon light irradiation (535 nm)
 1120 produces hydrogen by a synergistic effect of Ag NP and bR” [141]. Miao et al reviewed several applications
 1121 of 4D printing in membrane applications, examples are those using light and heat as stimuli [142]. In

1122 particular interest is the 4D printing of smart membranes, where the pores of the membranes can close or
1123 open, or the surface wettability can turn into hydrophilic or hydrophobic, depending on the external stimuli
1124 applied such as temperature change, pH change or some other parametric/stimuli changes.
1125

1126 **6. Conclusion**

1127 3D printing technology presents a high potential for use in various prototyping and fabrication processes
1128 including water-related applications. It is fast, versatile and efficient, which can fabricate virtually any shape
1129 and geometry enabling a new paradigm in the manufacturing industry. This review presented an overview
1130 of exciting developments in 3D-printed materials in the water-related field including preparation and use
1131 of feed channel spacers, membranes, solar absorbers, bio-carriers for wastewater treatment, adsorbents
1132 for oil-water separation and heavy metal treatment, desalination, among others. It is emphasized that in
1133 most water-related applications with macro-level materials (>1 μm range), the use of 3D printing is most
1134 suitable as it offers more degrees of freedom in design. However, those needing below 1 μm range
1135 resolution are still facing challenges in precision fabrication of materials especially on direct printing of
1136 membranes. Key areas that need to be further investigated and improved are on the printing
1137 resolution/accuracy, applicability of various materials for printing, printing speed and scalability, and the
1138 total cost of the process. The exciting hybridization of 3D printing with other fabrication processes may
1139 allow production of more novel designs and functionalities. Making the 3D printed material to be
1140 responsive to stimuli via 4D printing will open new horizons of research and further applications. Overall,
1141 the exciting field of 3D printing as a manufacturing technique is a new paradigm in new material design and
1142 fabrication that have wide promise in water-related applications. There is already a drastic advancement
1143 in the last few years in 3D printing, however, some 3D printing material, process, cost and post-processing
1144 parameters and even its environmental and health impacts needs to be addressed in order to fully realize
1145 its unlimited potential.

1146 **Conflict of interest**

1147 Authors hereby confirm that this manuscript has not been published and is not under consideration
1148 elsewhere. Authors declare no conflict of interest.

1151 **Acknowledgements**

1152 Leonard Tijing is grateful for the Centre for Technology in Water and Wastewater internal fund support.
1153 John Ryan Dizon and Rigoberto Advincula both acknowledge support from the Department of Science and
1154 Technology – PCIEERD Program and the DOST-AMCen, Philippines in various endeavours related to 3D
1155 printing processes and materials. Ho Kyong Shon thanks the support from his ARC Future Fellowship
1156 (FT140101208).
1157
1158

1159 **References**

- 1161 [1] P.J.J. Alvarez, C.K. Chan, M. Elimelech, N.J. Halas, D. Villagrán, Emerging opportunities for
1162 nanotechnology to enhance water security, *Nature Nanotechnology* 13(8) (2018) 634-641.
1163 [2] T.D. Ngo, A. Kashani, G. Imbalzano, K.T.Q. Nguyen, D. Hui, Additive manufacturing (3D printing): A
1164 review of materials, methods, applications and challenges, *Composites Part B: Engineering* 143 (2018)
1165 172-196.
1166 [3] J.-Y. Lee, W.S. Tan, J. An, C.K. Chua, C.Y. Tang, A.G. Fane, T.H. Chong, The potential to enhance
1167 membrane module design with 3D printing technology, *Journal of Membrane Science* 499 (2016) 480-
1168 490.
1169 [4] J.-Y. Lee, J. An, C.K. Chua, Fundamentals and applications of 3D printing for novel materials, *Applied*
1170 *Materials Today* 7 (2017) 120-133.

1171 [5] M.L. Perrotta, G. Saielli, G. Casella, F. Macedonio, L. Giorno, E. Drioli, A. Gugliuzza, An ultrathin
1172 suspended hydrophobic porous membrane for high-efficiency water desalination, *Applied Materials*
1173 *Today* 9 (2017) 1-9.

1174 [6] F. Li, W. Meindersma, A.B. de Haan, T. Reith, Novel spacers for mass transfer enhancement in
1175 membrane separations, *Journal of Membrane Science* 253(1) (2005) 1-12.

1176 [7] N. Sreedhar, N. Thomas, O. Al-Ketan, R. Rowshan, H. Hernandez, R.K. Abu Al-Rub, H.A. Arafat, 3D
1177 printed feed spacers based on triply periodic minimal surfaces for flux enhancement and biofouling
1178 mitigation in RO and UF, *Desalination* 425 (2018) 12-21.

1179 [8] N. Thomas, N. Sreedhar, O. Al-Ketan, R. Rowshan, R.K. Abu Al-Rub, H. Arafat, 3D printed spacers based
1180 on TPMS architectures for scaling control in membrane distillation, *Journal of Membrane Science* 581
1181 (2019) 38-49.

1182 [9] N. Yanar, M. Son, E. Yang, Y. Kim, H. Park, S.-E. Nam, H. Choi, Investigation of the performance
1183 behavior of a forward osmosis membrane system using various feed spacer materials fabricated by 3D
1184 printing technique, *Chemosphere* 202 (2018) 708-715.

1185 [10] T. Femmer, A.J.C. Kuehne, J. Torres-Rendon, A. Walther, M. Wessling, Print your membrane: Rapid
1186 prototyping of complex 3D-PDMS membranes via a sacrificial resist, *Journal of Membrane Science* 478
1187 (2015) 12-18.

1188 [11] L.C. Hwa, M.B. Uday, N. Ahmad, A.M. Noor, S. Rajoo, K.B. Zakaria, Integration and fabrication of the
1189 cheap ceramic membrane through 3D printing technology, *Materials Today Communications* 15 (2018)
1190 134-142.

1191 [12] A. Al-Shimmery, S. Mazinani, J. Ji, Y.M.J. Chew, D. Mattia, 3D printed composite membranes with
1192 enhanced anti-fouling behaviour, *Journal of Membrane Science* 574 (2019) 76-85.

1193 [13] Z.-X. Low, Y.T. Chua, B.M. Ray, D. Mattia, I.S. Metcalfe, D.A. Patterson, Perspective on 3D printing of
1194 separation membranes and comparison to related unconventional fabrication techniques, *Journal of*
1195 *Membrane Science* 523 (2017) 596-613.

1196 [14] L. Hu, G. Jiang, 3D Printing Techniques in Environmental Science and Engineering Will Bring New
1197 Innovation, *Environmental Science & Technology* 51(7) (2017) 3597-3599.

1198 [15] H.A. Balogun, R. Sulaiman, S.S. Marzouk, A. Giwa, S.W. Hasan, 3D printing and surface imprinting
1199 technologies for water treatment: A review, *Journal of Water Process Engineering* 31 (2019) 100786.

1200 [16] I.A. 52915:2016, I. 261 A. Manufacturing, <https://www.iso.org/standard/67472.html> Accessed: 23-
1201 Jun-2019 (2016).

1202 [17] A.C. de Leon, Q. Chen, N.B. Palaganas, J.O. Palaganas, J. Manapat, R.C. Advincula, High performance
1203 polymer nanocomposites for additive manufacturing applications, *Reactive and Functional Polymers* 103
1204 (2016) 141-155.

1205 [18] J.R.C. Dizon, A.H. Espera, Q. Chen, R.C. Advincula, Mechanical characterization of 3D-printed
1206 polymers, *Additive Manufacturing* 20 (2018) 44-67.

1207 [19] A.H. Espera, J.R.C. Dizon, Q. Chen, R.C. Advincula, 3D-printing and advanced manufacturing for
1208 electronics, *Progress in Additive Manufacturing* (2019).

1209 [20] K. Gnanasekaran, T. Heijmans, S. van Bennekom, H. Woldhuis, S. Wijnia, G. de With, H. Friedrich, 3D
1210 printing of CNT- and graphene-based conductive polymer nanocomposites by fused deposition modeling,
1211 *Applied Materials Today* 9 (2017) 21-28.

1212 [21] M. Vaezi, H. Seitz, S. Yang, A review on 3D micro-additive manufacturing technologies, *The*
1213 *International Journal of Advanced Manufacturing Technology* 67(5) (2013) 1721-1754.

1214 [22] X. Wang, M. Jiang, Z. Zhou, J. Gou, D. Hui, 3D printing of polymer matrix composites: A review and
1215 prospective, *Composites Part B: Engineering* 110 (2017) 442-458.

1216 [23] S. Crump, Fast, Precise, Safe Prototype with FDM, *ASME PED* 50 (1991) 53-60.

1217 [24] A.K. Sood, R.K. Ohdar, S.S. Mahapatra, Parametric appraisal of mechanical property of fused
1218 deposition modelling processed parts, *Materials & Design* 31(1) (2010) 287-295.

1219 [25] A. Tsouknidas, Friction Induced Wear of Rapid Prototyping Generated Materials: A Review, *Advances*
1220 *in Tribology* 2011 (2011) 7.

1221 [26] J.M. Williams, A. Adewunmi, R.M. Schek, C.L. Flanagan, P.H. Krebsbach, S.E. Feinberg, S.J. Hollister, S.
1222 Das, Bone tissue engineering using polycaprolactone scaffolds fabricated via selective laser sintering,
1223 *Biomaterials* 26(23) (2005) 4817-4827.

1224 [27] S. Kumar, J.-P. Kruth, Wear Performance of SLS/SLM Materials, *Advanced Engineering Materials* 10(8)
1225 (2008) 750-753.

1226 [28] G.D. Kim, Y.T. Oh, A benchmark study on rapid prototyping processes and machines: Quantitative
1227 comparisons of mechanical properties, accuracy, roughness, speed, and material cost, *Proceedings of the*
1228 *Institution of Mechanical Engineers, Part B: Journal of Engineering Manufacture* 222(2) (2008) 201-215.

1229 [29] C. Deckard, J.J. Beaman, Process and control issues in selective laser sintering, *American Society of*
1230 *Mechanical Engineers, Production Engineering Division (Publication) PED*, 1988, pp. 191-197.

1231 [30] I. Gibson, Material properties and fabrication parameters in selective laser sintering process, *Rapid*
1232 *Prototyping Journal* 3(4) (1997) 129-136.

1233 [31] N. Thomas, N. Sreedhar, O. Al-Ketan, R. Rowshan, R.K. Abu Al-Rub, H. Arafat, 3D printed triply
1234 periodic minimal surfaces as spacers for enhanced heat and mass transfer in membrane distillation,
1235 *Desalination* 443 (2018) 256-271.

1236 [32] E.H.C. Castillo, N. Thomas, O. Al-Ketan, R. Rowshan, R.K. Abu Al-Rub, L.D. Nghiem, S. Vigneswaran,
1237 H.A. Arafat, G. Naidu, 3D printed spacers for organic fouling mitigation in membrane distillation, *Journal*
1238 *of Membrane Science* 581 (2019) 331-343.

1239 [33] W.S. Tan, C.K. Chua, T.H. Chong, A.G. Fane, A. Jia, 3D printing by selective laser sintering of
1240 polypropylene feed channel spacers for spiral wound membrane modules for the water industry, *Virtual*
1241 *and Physical Prototyping* 11(3) (2016) 151-158.

1242 [34] W.S. Tan, S.R. Suwarno, J. An, C.K. Chua, A.G. Fane, T.H. Chong, Comparison of solid, liquid and
1243 powder forms of 3D printing techniques in membrane spacer fabrication, *Journal of Membrane Science*
1244 537 (2017) 283-296.

1245 [35] A. Siddiqui, N. Farhat, S.S. Bucs, R.V. Linares, C. Picioreanu, J.C. Kruithof, M.C.M. van Loosdrecht, J.
1246 Kidwell, J.S. Vrouwenvelder, Development and characterization of 3D-printed feed spacers for spiral
1247 wound membrane systems, *Water Research* 91 (2016) 55-67.

1248 [36] Y.Z. Tan, Z. Mao, Y. Zhang, W.S. Tan, T.H. Chong, B. Wu, J.W. Chew, Enhancing fouling mitigation of
1249 submerged flat-sheet membranes by vibrating 3D-spacers, *Separation and Purification Technology* 215
1250 (2019) 70-80.

1251 [37] S. Kerdi, A. Qamar, J.S. Vrouwenvelder, N. Ghaffour, Fouling resilient perforated feed spacers for
1252 membrane filtration, *Water Research* 140 (2018) 211-219.

1253 [38] J. Balster, I. Pünt, D.F. Stamatialis, M. Wessling, Multi-layer spacer geometries with improved mass
1254 transport, *Journal of Membrane Science* 282(1) (2006) 351-361.

1255 [39] A. Shrivastava, S. Kumar, E.L. Cussler, Predicting the effect of membrane spacers on mass transfer,
1256 *Journal of Membrane Science* 323(2) (2008) 247-256.

1257 [40] J. Liu, A. Iranshahi, Y. Lou, G. Lipscomb, Static mixing spacers for spiral wound modules, *Journal of*
1258 *Membrane Science* 442 (2013) 140-148.

1259 [41] C. Fritzmman, M. Hausmann, M. Wiese, M. Wessling, T. Melin, Microstructured spacers for
1260 submerged membrane filtration systems, *Journal of Membrane Science* 446 (2013) 189-200.

1261 [42] C. Fritzmman, M. Wiese, T. Melin, M. Wessling, Helically microstructured spacers improve mass
1262 transfer and fractionation selectivity in ultrafiltration, *Journal of Membrane Science* 463 (2014) 41-48.

1263 [43] S.M. Ali, A. Qamar, S. Kerdi, S. Phuntsho, J.S. Vrouwenvelder, N. Ghaffour, H.K. Shon, Energy efficient
1264 3D printed column type feed spacer for membrane filtration, *Water Research* 164 (2019) 114961.

1265 [44] S. Badalov, Y. Oren, C.J. Arnusch, Ink-jet printing assisted fabrication of patterned thin film composite
1266 membranes, *Journal of Membrane Science* 493 (2015) 508-514.

1267 [45] S. Mazinani, A. Al-Shimmery, Y.M.J. Chew, D. Mattia, 3D Printed Fouling-Resistant Composite
1268 Membranes, *ACS Applied Materials & Interfaces* (2019).

1269 [46] Y. Chen, P. Gao, M.J. Summe, W.A. Phillip, N. Wei, Biocatalytic membranes prepared by inkjet
1270 printing functionalized yeast cells onto microfiltration substrates, *Journal of Membrane Science* 550
1271 (2018) 91-100.

1272 [47] M. Singh, A.P. Haring, Y. Tong, E. Cesewski, E. Ball, R. Jasper, E.M. Davis, B.N. Johnson, Additive
1273 Manufacturing of Mechanically Isotropic Thin Films and Membranes via Microextrusion 3D Printing of
1274 Polymer Solutions, *ACS Applied Materials & Interfaces* 11(6) (2019) 6652-6661.

1275 [48] M.R. Chowdhury, J. Steffes, B.D. Huey, J.R. McCutcheon, 3D printed polyamide membranes for
1276 desalination, *Science* 361(6403) (2018) 682-686.

1277 [49] S. Yuan, D. Strobbe, J.-P. Kruth, P. Van Puyvelde, B. Van der Bruggen, Super-hydrophobic 3D printed
1278 polysulfone membranes with a switchable wettability by self-assembled candle soot for efficient gravity-
1279 driven oil/water separation, *Journal of Materials Chemistry A* 5(48) (2017) 25401-25409.

1280 [50] S. Yuan, J. Zhu, Y. Li, Y. Zhao, J. Li, P. Van Puyvelde, B. Van der Bruggen, Structure architecture of
1281 micro/nanoscale ZIF-L on a 3D printed membrane for a superhydrophobic and underwater
1282 superoleophobic surface, *Journal of Materials Chemistry A* 7(6) (2019) 2723-2729.

1283 [51] J. Seo, D.I. Kushner, M.A. Hickner, 3D Printing of Micropatterned Anion Exchange Membranes, *ACS*
1284 *Applied Materials & Interfaces* 8(26) (2016) 16656-16663.

1285 [52] M. Czölderová, M. Behúl, J. Filip, P. Zajíček, R. Grabic, A. Vojs-Staňová, M. Gál, K. Kerekeš, J. Híveš, J.
1286 Ryba, M. Rybanská, P. Brandeburová, T. Mackuľák, 3D printed polyvinyl alcohol ferrate(VI) capsules:
1287 Effective means for the removal of pharmaceuticals and illicit drugs from wastewater, *Chemical*
1288 *Engineering Journal* 349 (2018) 269-275.

1289 [53] Y. Dong, S.-Q. Fan, Y. Shen, J.-X. Yang, P. Yan, Y.-P. Chen, J. Li, J.-S. Guo, X.-M. Duan, F. Fang, S.-Y. Liu,
1290 A Novel Bio-carrier Fabricated Using 3D Printing Technique for Wastewater Treatment, *Scientific Reports*
1291 5 (2015) 12400.

1292 [54] O. Elliott, S. Gray, M. McClay, B. Nassief, A. Nunnolley, E. Vogt, J. Ekong, K. Kardel, A. Khoshkhoo, G.
1293 Proaño, D.M. Blesch, A.L. Carrano, Design and Manufacturing of High Surface Area 3D-Printed Media for
1294 Moving Bed Bioreactors for Wastewater Treatment, *Journal of Contemporary Water Research &*
1295 *Education* 160(1) (2017) 144-156.

1296 [55] Y. Li, T. Gao, Z. Yang, C. Chen, W. Luo, J. Song, E. Hitz, C. Jia, Y. Zhou, B. Liu, B. Yang, L. Hu, 3D-Printed,
1297 All-in-One Evaporator for High-Efficiency Solar Steam Generation under 1 Sun Illumination, *Advanced*
1298 *Materials* 29(26) (2017) 1700981.

1299 [56] Y. Li, T. Gao, Z. Yang, C. Chen, Y. Kuang, J. Song, C. Jia, E.M. Hitz, B. Yang, L.J.N.E. Hu, Graphene oxide-
1300 based evaporator with one-dimensional water transport enabling high-efficiency solar desalination, 41
1301 (2017) 201-209.

1302 [57] P. He, X. Tang, L. Chen, P. Xie, L. He, H. Zhou, D. Zhang, T.J.A.F.M. Fan, Patterned Carbon Nitride-
1303 Based Hybrid Aerogel Membranes via 3D Printing for Broadband Solar Wastewater Remediation, 28(29)
1304 (2018) 1801121.

1305 [58] Z. Wang, J. Wang, M. Li, K. Sun, C.-j.J.S.r. Liu, Three-dimensional printed acrylonitrile butadiene
1306 styrene framework coated with Cu-BTC metal-organic frameworks for the removal of methylene blue, 4
1307 (2014) 5939.

1308 [59] A. Figuerola, D.A. Medina, A.J. Santos-Neto, C.P. Cabello, V. Cerdà, G.T. Palomino, F.J.A.M.T. Maya,
1309 Metal-organic framework mixed-matrix coatings on 3D printed devices, 16 (2019) 21-27.

1310 [60] Y. Yang, X. Li, X. Zheng, Z. Chen, Q. Zhou, Y. Chen, 3D-Printed Biomimetic Super-Hydrophobic
1311 Structure for Microdroplet Manipulation and Oil/Water Separation, *Advanced Materials* 30(9) (2018)
1312 1704912.

1313 [61] C. Yan, Z. Ji, S. Ma, X. Wang, F. Zhou, 3D Printing as Feasible Platform for On-Site Building Oil-
1314 Skimmer for Oil Collection from Spills, *Advanced Materials Interfaces* 3(13) (2016) 1600015.

1315 [62] Z. Chen, D. Zhang, E. Peng, J. Ding, 3D-printed ceramic structures with in situ grown whiskers for
1316 effective oil/water separation, *Chemical Engineering Journal* 373 (2019) 1223-1232.

1317 [63] J. Lv, Z. Gong, Z. He, J. Yang, Y. Chen, C. Tang, Y. Liu, M. Fan, W.-M. Lau, 3D printing of a mechanically
1318 durable superhydrophobic porous membrane for oil-water separation, *Journal of Materials Chemistry A*
1319 5(24) (2017) 12435-12444.

1320 [64] A.R. Da Costa, A.G. Fane, D.E. Wiley, Spacer characterization and pressure drop modelling in spacer-
1321 filled channels for ultrafiltration, *Journal of Membrane Science* 87(1) (1994) 79-98.

1322 [65] A.R. Da Costa, A.G. Fane, C.J.D. Fell, A.C.M. Franken, Optimal channel spacer design for ultrafiltration,
1323 *Journal of Membrane Science* 62(3) (1991) 275-291.

1324 [66] W.M. F. Li, A. de Haan, T. Reith, Spacer for use in a membrane separation device and a membrane
1325 separation device comprising such a spacer,, *World Intellectual Property Organization* (2004) WO
1326 2004/112945 A1.

1327 [67] J.R. Werber, C.O. Osuji, M. Elimelech, Materials for next-generation desalination and water
1328 purification membranes, *Nature Reviews Materials* 1 (2016) 16018.

1329 [68] Y. Ying, W. Ying, Q. Li, D. Meng, G. Ren, R. Yan, X. Peng, Recent advances of nanomaterial-based
1330 membrane for water purification, *Applied Materials Today* 7 (2017) 144-158.

1331 [69] Y.C. Woo, Y. Kim, M. Yao, L.D. Tijing, J.-S. Choi, S. Lee, S.-H. Kim, H.K. Shon, Hierarchical composite
1332 membranes with robust omniphobic surface using layer-by-layer assembly technique, *Environmental*
1333 *science & technology* 52(4) (2018) 2186-2196.

1334 [70] M. Yao, J. Ren, N. Akther, Y.C. Woo, L.D. Tijing, S.-H. Kim, H.K. Shon, Improving membrane distillation
1335 performance: Morphology optimization of hollow fiber membranes with selected non-solvent in dope
1336 solution, *Chemosphere* 230 (2019) 117-126.

1337 [71] L.D. Tijing, J.-S. Choi, S. Lee, S.-H. Kim, H.K. Shon, Recent progress of membrane distillation using
1338 electrospun nanofibrous membrane, *Journal of Membrane Science* 453 (2014) 435-462.

1339 [72] L.D. Tijing, Y.C. Woo, W.-G. Shim, T. He, J.-S. Choi, S.-H. Kim, H.K. Shon, Superhydrophobic nanofiber
1340 membrane containing carbon nanotubes for high-performance direct contact membrane distillation,
1341 *Journal of Membrane Science* 502 (2016) 158-170.

1342 [73] M. Yao, Y.C. Woo, L.D. Tijing, W.-G. Shim, J.-S. Choi, S.-H. Kim, H.K. Shon, Effect of heat-press
1343 conditions on electrospun membranes for desalination by direct contact membrane distillation,
1344 *Desalination* 378 (2016) 80-91.

1345 [74] L.D. Tijing, Y.C. Woo, J.-S. Choi, S. Lee, S.-H. Kim, H.K. Shon, Fouling and its control in membrane
1346 distillation—A review, *Journal of Membrane Science* 475 (2015) 215-244.

1347 [75] T. Femmer, A.J.C. Kuehne, M. Wessling, Print your own membrane: direct rapid prototyping of
1348 polydimethylsiloxane, *Lab on a Chip* 14(15) (2014) 2610-2613.

1349 [76] A.N. Sue Mecham, Rima Januszewicz, Benny D. Freeman and Joseph M. DeSimone, Continuous liquid
1350 interface production (CLIP) of precise membrane structures, North American Membrane Society Meeting,
1351 Boston, USA, 2015.

1352 [77] W. Lin, Enhanced continuous liquid interface production with track-etched membrane, *Rapid*
1353 *Prototyping Journal* 25(1) (2019) 117-125.

1354 [78] L. Hernandez-Afonso, R. Fernandez-Gonzalez, P. Esparza, M.E. Borges, S. Diaz Gonzalez, J. Canales-
1355 Vasquez, J.C. Ruiz-Morales, Ceramic-Based 3D Printed Supports for Photocatalytic Treatment of
1356 Wastewater, *Journal of Chemistry* 2017 (2017) 9.

1357 [79] A. Kudo, Y.J.C.S.R. Miseki, Heterogeneous photocatalyst materials for water splitting, 38(1) (2009)
1358 253-278.

1359 [80] A. Vyatskikh, A. Kudo, S. Delalande, J.R.J.M.T.C. Greer, Additive manufacturing of polymer-derived
1360 titania for one-step solar water purification, 15 (2018) 288-293.

1361 [81] A. Sangiorgi, Z. Gonzalez, A. Ferrandez-Montero, J. Yus, A. Sanchez-Herencia, C. Galassi, A. Sanson,
1362 B.J.J.o.T.E.S. Ferrari, 3D Printing of Photocatalytic Filters Using a Biopolymer to Immobilize TiO₂
1363 Nanoparticles, 166(5) (2019) H3239-H3248.

1364 [82] M.J.M. de Vidales, A. Nieto-Márquez, D. Morcuende, E. Atanes, F. Blaya, E. Soriano, F.J.C.T.
1365 Fernández-Martínez, 3D printed floating photocatalysts for wastewater treatment, (2019).

1366 [83] A. Vyatskikh, A. Kudo, S. Delalande, J.R. Greer, Additive manufacturing of polymer-derived titania for
1367 one-step solar water purification, *Materials Today Communications* 15 (2018) 288-293.

1368 [84] Y. de Rancourt de Mimérand, K. Li, J. Guo, Photoactive Hybrid Materials with Fractal Designs
1369 Produced via 3D Printing and Plasma Grafting Technologies, *ACS Applied Materials & Interfaces* 11(27)
1370 (2019) 24771-24781.

1371 [85] X. Zhou, C.-j. Liu, Three-dimensional Printing for Catalytic Applications: Current Status and
1372 Perspectives, *Advanced Functional Materials* 27(30) (2017) 1701134.

1373 [86] Prabhat K. Rai, J. Lee, S.K. Kailasa, E.E. Kwon, Y.F. Tsang, Y.S. Ok, K.-H. Kim, A critical review of
1374 ferrate(VI)-based remediation of soil and groundwater, *Environmental Research* 160 (2018) 420-448.

1375 [87] B. Yuan, Y. Chen, M.-L. Fu, Degradation efficiencies and mechanisms of trichloroethylene (TCE) by
1376 controlled-release permanganate (CRP) oxidation, *Chemical Engineering Journal* 192 (2012) 276-283.

1377 [88] K. Biswas, Taylor, M.W. & Turner, S.J., Successional development of biofilms in moving bed biofilm
1378 reactor (MBBR) systems treating municipal wastewater, *Appl Microbiol Biotechnol* 98 (2014) 1429.

1379 [89] B. Tang, Y. Zhao, L. Bin, S. Huang, F. Fu, Variation of the characteristics of biofilm on the semi-
1380 suspended bio-carrier produced by a 3D printing technique: Investigation of a whole growing cycle,
1381 *Bioresource Technology* 244 (2017) 40-47.

1382 [90] B. Tang, H. Song, L. Bin, S. Huang, W. Zhang, F. Fu, Y. Zhao, Q. Chen, Determination of the profile of
1383 DO and its mass transferring coefficient in a biofilm reactor packed with semi-suspended bio-carriers,
1384 *Bioresource Technology* 241 (2017) 54-62.

1385 [91] Z. Jiang, L.D. Tijing, A. Amarjargal, C.H. Park, K.-J. An, H.K. Shon, C.S. Kim, Removal of oil from water
1386 using magnetic bicomponent composite nanofibers fabricated by electrospinning, *Composites Part B:
1387 Engineering* 77 (2015) 311-318.

1388 [92] J.H. Shin, J.-H. Heo, S. Jeon, J.H. Park, S. Kim, H.-W. Kang, Bio-inspired hollow PDMS sponge for
1389 enhanced oil–water separation, *Journal of Hazardous Materials* 365 (2019) 494-501.

1390 [93] R. Xing, B. Yang, R. Huang, W. Qi, R. Su, B.P. Binks, Z. He, Three-Dimensionally Printed Bioinspired
1391 Superhydrophobic Packings for Oil-in-Water Emulsion Separation, *Langmuir* 35(39) (2019) 12799-12806.

1392 [94] P.J.E.S.N. Wang, Emerging investigator series: the rise of nano-enabled photothermal materials for
1393 water evaporation and clean water production by sunlight, 5(5) (2018) 1078-1089.

1394 [95] Y.-S. Jun, X. Wu, D. Ghim, Q. Jiang, S. Cao, S.J.A.o.c.r. Singamaneni, Photothermal Membrane Water
1395 Treatment for Two Worlds, (2019).

1396 [96] Y. Li, T. Gao, Z. Yang, C. Chen, W. Luo, J. Song, E. Hitz, C. Jia, Y. Zhou, B.J.A.M. Liu, 3D-printed, all-in-
1397 one evaporator for high-efficiency solar steam generation under 1 sun illumination, 29(26) (2017)
1398 1700981.

1399 [97] Y. Li, T. Gao, Z. Yang, C. Chen, Y. Kuang, J. Song, C. Jia, E.M. Hitz, B. Yang, L. Hu, Graphene oxide-based
1400 evaporator with one-dimensional water transport enabling high-efficiency solar desalination, *Nano
1401 Energy* 41 (2017) 201-209.

1402 [98] K. Fu, Y. Yao, J. Dai, L.J.A.M. Hu, Progress in 3D printing of carbon materials for energy-related
1403 applications, 29(9) (2017) 1603486.

1404 [99] E.B. Secor, M.C. Hersam, Emerging Carbon and Post-Carbon Nanomaterial Inks for Printed
1405 Electronics, *The Journal of Physical Chemistry Letters* 6(4) (2015) 620-626.

1406 [100] F. Torrisi, T. Hasan, W. Wu, Z. Sun, A. Lombardo, T.S. Kulmala, G.-W. Hsieh, S. Jung, F. Bonaccorso,
1407 P.J. Paul, D. Chu, A.C. Ferrari, Inkjet-Printed Graphene Electronics, *ACS Nano* 6(4) (2012) 2992-3006.

1408 [101] A. Kamyshny, S. Magdassi, Conductive Nanomaterials for Printed Electronics, 10(17) (2014) 3515-
1409 3535.

1410 [102] P. Zhang, Q. Liao, H. Yao, H. Cheng, Y. Huang, C. Yang, L. Jiang, L. Qu, Three-dimensional water
1411 evaporation on a macroporous vertically aligned graphene pillar array under one sun, *Journal of Materials
1412 Chemistry A* 6(31) (2018) 15303-15309.

1413 [103] Z. Liu, X. Zhou, C.-j.J.D. Liu, R. Materials, N-doped porous carbon material prepared via direct ink
1414 writing for the removal of methylene blue, 95 (2019) 121-126.

1415 [104] Y. Wang, X. Ling, Y. Wang, J.J.D. Zhang, R. Materials, Probing the effect of doped F and N on the
1416 structures and properties of fullerene-like hydrogenated carbon films, 79 (2017) 32-37.

1417 [105] A.D. Valino, J.R.C. Dizon, A.H. Espera, Q. Chen, J. Messman, R.C. Advincula, Advances in 3D printing
1418 of thermoplastic polymer composites and nanocomposites, *Progress in Polymer Science* 98 (2019)
1419 101162.

1420 [106] D. Zhang, J. Xiao, Q. Guo, J.J.J.o.M.S. Yang, 3D-printed highly porous and reusable chitosan
1421 monoliths for Cu(II) removal, 54(8) (2019) 6728-6741.

1422 [107] Y. Hu, X. Liu, J. Bai, K. Shih, E.Y. Zeng, H.J.E.S. Cheng, P. Research, Assessing heavy metal pollution in
1423 the surface soils of a region that had undergone three decades of intense industrialization and
1424 urbanization, 20(9) (2013) 6150-6159.

1425 [108] D. Zhang, J. Xiao, Q. Guo, J.J.J.o.M.S. Yang, 3D-printed highly porous and reusable chitosan
1426 monoliths for Cu (II) removal, 54(8) (2019) 6728-6741.

1427 [109] G.A. Appuhamillage, D.R. Berry, C.E. Benjamin, M.A. Luzuriaga, J.C. Reagan, J.J. Gassensmith, R.A.
1428 Smaldone, A biopolymer-based 3D printable hydrogel for toxic metal adsorption from water, *Polymer
1429 International* 68(5) (2019) 964-971.

1430 [110] P. Sun, L. Zhang, S. Tao, Preparation of hybrid chitosan membranes by selective laser sintering for
1431 adsorption and catalysis, *Materials & Design* 173 (2019) 107780.

1432 [111] F. Niesler, M. Hermatschweiler, Two-Photon Polymerization — A Versatile Microfabrication Tool,
1433 *Laser Technik Journal* 12(3) (2015) 44-47.

- 1434 [112] J.R.C. Dizon, Q. Chen, A.D. Valino, R.C. Advincula, Thermo-mechanical and swelling properties of
 1435 three-dimensional-printed poly (ethylene glycol) diacrylate/silica nanocomposites, *MRS Communications*
 1436 9(1) (2019) 209-217.
- 1437 [113] J.R. Tumbleston, D. Shirvanyants, N. Ermoshkin, R. Januszewicz, A.R. Johnson, D. Kelly, K. Chen, R.
 1438 Pinschmidt, J.P. Rolland, A. Ermoshkin, E.T. Samulski, J.M. DeSimone, Continuous liquid interface
 1439 production of 3D objects, *Science* 347(6228) (2015) 1349-1352.
- 1440 [114] A.J. Scardino, H. Zhang, D.J. Cookson, R.N. Lamb, R.d. Nys, The role of nano-roughness in antifouling,
 1441 *Biofouling* 25(8) (2009) 757-767.
- 1442 [115] P. Azimi, D. Zhao, C. Pouzet, N.E. Crain, B. Stephens, Emissions of Ultrafine Particles and Volatile
 1443 Organic Compounds from Commercially Available Desktop Three-Dimensional Printers with Multiple
 1444 Filaments, *Environmental Science & Technology* 50(3) (2016) 1260-1268.
- 1445 [116] Y. Kim, C. Yoon, S. Ham, J. Park, S. Kim, O. Kwon, P.-J. Tsai, Emissions of Nanoparticles and Gaseous
 1446 Material from 3D Printer Operation, *Environmental Science & Technology* 49(20) (2015) 12044-12053.
- 1447 [117] P. Graff, B. Ståhlbom, E. Nordenberg, A. Graichen, P. Johansson, H. Karlsson, Evaluating Measuring
 1448 Techniques for Occupational Exposure during Additive Manufacturing of Metals: A Pilot Study, *Journal of*
 1449 *Industrial Ecology* 21(S1) (2017) S120-S129.
- 1450 [118] D.R. I. Gibson, and B. Stucker, *Additive manufacturing technologies: 3D printing, rapid prototyping,*
 1451 *and direct digital manufacturing (2nd ed)*, Springer2014.
- 1452 [119] J. Faludi, Comparing environmental impacts of additive manufacturing vs traditional machining via
 1453 life-cycle assessment, *Rapid Prototyping Journal* 21(1) (2015) 14-33.
- 1454 [120] R. LaSelle, Five critical shifts guiding the future of 3D printing, Retrieved from
 1455 [https://www.jabil.com/insights/blog-main/future-of-3d-printing-additive-manufacturing-looks-](https://www.jabil.com/insights/blog-main/future-of-3d-printing-additive-manufacturing-looks-bright.html)
 1456 [bright.html](https://www.jabil.com/insights/blog-main/future-of-3d-printing-additive-manufacturing-looks-bright.html) (2019).
- 1457 [121] S.A.M. Tofail, E.P. Koumoulos, A. Bandyopadhyay, S. Bose, L. O'Donoghue, C. Charitidis, Additive
 1458 manufacturing: scientific and technological challenges, market uptake and opportunities, *Materials Today*
 1459 21(1) (2018) 22-37.
- 1460 [122] L. Greguric, Can 3D printing be used for mass production?, Retrived from [https://all3dp.com/2/can-](https://all3dp.com/2/can-3d-printing-be-used-for-mass-production/)
 1461 [3d-printing-be-used-for-mass-production/](https://all3dp.com/2/can-3d-printing-be-used-for-mass-production/) (2019).
- 1462 [123] C. Schmidt, The future of additive manufacturing, Retrieved from
 1463 https://medium.com/@christina_39925/the-future-of-additive-manufacturing-6396d191183e (2018).
- 1464 [124] S.J. Lee, D.N. Heo, J.S. Park, S.K. Kwon, J.H. Lee, J.H. Lee, W.D. Kim, I.K. Kwon, S.A. Park,
 1465 Characterization and preparation of bio-tubular scaffolds for fabricating artificial vascular grafts by
 1466 combining electrospinning and a 3D printing system, *Physical Chemistry Chemical Physics* 17(5) (2015)
 1467 2996-2999.
- 1468 [125] I. Rajzer, A. Kurowska, A. Jabłoński, S. Jatteau, M. Śliwka, M. Ziąbka, E. Menaszek, Layered
 1469 gelatin/PLLA scaffolds fabricated by electrospinning and 3D printing- for nasal cartilages and subchondral
 1470 bone reconstruction, *Materials & Design* 155 (2018) 297-306.
- 1471 [126] S. Naghieh, E. Foroozmehr, M. Badrossamay, M. Kharaziha, Combinational processing of 3D printing
 1472 and electrospinning of hierarchical poly(lactic acid)/gelatin-forsterite scaffolds as a biocomposite:
 1473 Mechanical and biological assessment, *Materials & Design* 133 (2017) 128-135.
- 1474 [127] J.R.C. Dizon, Valino, A.D., Souza, L.R., Espera Jr., A.H., Chen, Q., Advincula, R.C. , 3D-Printed Molds
 1475 and Materials for Injection Molding and Rapid Tooling Applications, *MRS Communications* (2019 (Just
 1476 accepted)).
- 1477 [128] Large 3D printer ready to build, *Metal Powder Report* 74(3) (2019) 163-164.
- 1478 [129] F. Momeni, S. M.Mehdi Hassani.N, X. Liu, J. Ni, A review of 4D printing, *Materials & Design* 122
 1479 (2017) 42-79.
- 1480 [130] J. Zhou, S.S. Sheiko, Reversible shape-shifting in polymeric materials, *Journal of Polymer Science*
 1481 *Part B: Polymer Physics* 54(14) (2016) 1365-1380.
- 1482 [131] S. Tibbits, 4D Printing: Multi-Material Shape Change, *Architectural Design* 84(1) (2014) 116-121.
- 1483 [132] D. Raviv, W. Zhao, C. McKnelly, A. Papadopoulou, A. Kadambi, B. Shi, S. Hirsch, D. Dikovskiy, M.
 1484 Zyracki, C. Olguin, R. Raskar, S. Tibbits, Active Printed Materials for Complex Self-Evolving Deformations,
 1485 *Scientific Reports* 4 (2014) 7422.

1486 [133] M. Vaezi, S. Chianrabutra, B. Mellor, S. Yang, Multiple material additive manufacturing – Part 1: a
1487 review, *Virtual and Physical Prototyping* 8(1) (2013) 19-50.
1488 [134] Q. Ge, H.J. Qi, M.L. Dunn, Active materials by four-dimension printing, *Applied Physics Letters*
1489 103(13) (2013) 131901.
1490 [135] Q. Zhang, K. Zhang, G. Hu, Smart three-dimensional lightweight structure triggered from a thin
1491 composite sheet via 3D printing technique, *Scientific Reports* 6 (2016) 22431.
1492 [136] A. Sydney Gladman, E.A. Matsumoto, R.G. Nuzzo, L. Mahadevan, J.A. Lewis, Biomimetic 4D printing,
1493 *Nature Materials* 15 (2016) 413.
1494 [137] O. Kuksenok, A.C. Balazs, Stimuli-responsive behavior of composites integrating thermo-responsive
1495 gels with photo-responsive fibers, *Materials Horizons* 3(1) (2016) 53-62.
1496 [138] G. Villar, A.D. Graham, H. Bayley, A Tissue-Like Printed Material, *Science* 340(6128) (2013) 48-52.
1497 [139] D. Kokkinis, M. Schaffner, A.R. Studart, Multimaterial magnetically assisted 3D printing of composite
1498 materials, *Nature Communications* 6 (2015) 8643.
1499 [140] M. Nadgorny, Z. Xiao, C. Chen, L.A. Connal, Three-Dimensional Printing of pH-Responsive and
1500 Functional Polymers on an Affordable Desktop Printer, *ACS Applied Materials & Interfaces* 8(42) (2016)
1501 28946-28954.
1502 [141] A.S. Mathews, S. Abraham, S.K. Kumaran, J. Fan, C. Montemagno, Bio nano ink for 4D printing
1503 membrane proteins, *RSC Advances* 7(66) (2017) 41429-41434.
1504 [142] S. Miao, N. Castro, M. Nowicki, L. Xia, H. Cui, X. Zhou, W. Zhu, S.-j. Lee, K. Sarkar, G. Vozzi, Y. Tabata,
1505 J. Fisher, L.G. Zhang, 4D printing of polymeric materials for tissue and organ regeneration, *Materials*
1506 *Today* 20(10) (2017) 577-591.
1507